Author/s:
Tessema, MB;Feng, S;Enosi Tuipulotu, D;Farrukee, R;Ngo, C;Gago da Graça, C;Yamomoto, M;Utzschneider, DT;Brooks, AG;Londrigan, SL;Man, SM;Reading, PC

Title:
Mouse guanylate-binding proteins of the chromosome 3 cluster do not mediate antiviral activity in vitro or in mouse models of infection

Date:
2024-12-01

Citation:
Tessema, M. B., Feng, S., Enosi Tuipulotu, D., Farrukee, R., Ngo, C., Gago da Graça, C., Yamomoto, M., Utzschneider, D. T., Brooks, A. G., Londrigan, S. L., Man, S. M. & Reading, P. C. (2024). Mouse guanylate-binding proteins of the chromosome 3 cluster do not mediate antiviral activity in vitro or in mouse models of infection. Communications Biology, 7 (1), https://doi.org/10.1038/s42003-024-06748-8.

Persistent Link:
https://hdl.handle.net/11343/358445

communications biology

Article

https://doi.org/10.1038/s42003-024-06748-8

Mouse guanylate-binding proteins of the chromosome 3 cluster do not mediate antiviral activity in vitro or in mouse models of infection

Check for updates

Melkamu B. Tessema[1,5], Shouya Feng[2,6], Daniel Enosi Tuipulotu[2,7], Rubaiyea Farrukee[1], Chinh Ngo[2], Catarina Gago da Graça[1], Masahiro Yamomoto[3], Daniel T. Utzschneider[1], Andrew G. Brooks[1], Sarah L. Londrigan[1], Si Ming Man[2] & Patrick C. Reading[1,4] ✉

Dynamin-like GTPase proteins, including myxoma (Mx) and guanylate-binding proteins (GBPs), are among the many interferon stimulated genes induced following viral infections. While studies report that human (h)GBPs inhibit different viruses in vitro, few have convincingly demonstrated that mouse (m)GBPs mediate antiviral activity, although mGBP-deficient mice have been used extensively to define their importance in immunity to diverse intracellular bacteria and protozoa. Herein, we demonstrate that individual (overexpression) or collective (knockout (KO) mice) mGBPs of the chromosome 3 cluster (mGBPchr3) do not inhibit replication of five viruses from different virus families in vitro, nor do we observe differences in virus titres recovered from wild type versus mGBPchr3 KO mice after infection with three of these viruses (influenza A virus, herpes simplex virus type 1 or lymphocytic choriomeningitis virus). These data indicate that mGBPchr3 do not appear to be a major component of cell-intrinsic antiviral immunity against the diverse viruses tested in our studies.

The dynamin-like GTPase family of proteins are interferon (IFN)-inducible proteins which include guanylate-binding proteins (GBPs), myxovirus resistance (Mx) proteins, and the immunity related GTPases (IRG). To date, 7 human and 11 mouse GBPs have been described with all human (h)GBPs localised to chromosome 1 and mouse (m)GBPs mapped to chromosomes 3 (*Gbp1*, *Gbp2*, *Gbp3*, *Gbp5*, *Gbp7* and one pseudogene) and 5 (*Gbp4*, *Gbp6*, *Gbp8*, *Gbp9*, *Gbp10*, *Gbp11* and another pseudogene) (reviewed in ref. 1). In general terms, GBPs exhibit GTPase activity, oligomerization and membrane-binding ability with each function attributed to a distinct GBP domain and functions tend to be dependent on one another for optimum efficiency[2]. For example, GTP-binding stimulates oligomerization of GBPs which, in turn, enhances their enzymatic activity[3–5], while subcellular localization and membrane-associated functions can also be boosted following oligomerization[6]. Moreover, these functions contribute to their potent activity against a range of intracellular bacteria and protozoa (reviewed in ref. 7).

Since Anderson et al. first demonstrated that constitutive over-expression of human (h)GBP1 in HeLa cells reduced titres of vesicular stomatitis virus (VSV) or encephalomyocarditis virus (EMCV) by ~50% compared to those from parental cells[8], subsequent in vitro studies have demonstrated that a number of hGBPs can mediate antiviral activity against particular viruses in vitro (reviewed in ref. 9). For example, hGBP1 inhibits replication of a number of viruses, including Kaposi's sarcoma-associated herpesvirus (KSHV)[10], Classical Swine Fever Virus (CSFV)[11] and influenza A virus (IAV)[12,13], although antiviral activity was reported to be antagonized by the NS5A protein of CSFV[11] and the NS1 protein of IAV[13]. hGBP3 and a

[1]Department of Microbiology and Immunology, University of Melbourne, at The Peter Doherty Institute for Infection and Immunity, 792 Elizabeth St, Victoria, 3000, Australia. [2]Division of Immunology and Infectious Disease, The John Curtin School of Medical Research, The Australian National University, Canberra, Australia. [3]Department of Immunoparasitology, Research Institute for Microbial Diseases, Osaka University, Osaka, Japan. [4]WHO Collaborating Centre for Reference and Research on Influenza, Victorian Infectious Diseases Reference Laboratory, at The Peter Doherty Institute for Infection and Immunity, 792 Elizabeth St, Victoria, 3000, Australia. [5]Present address: WHO Collaborating Centre for Reference and Research on Influenza, Victorian Infectious Diseases Reference Laboratory, at The Peter Doherty Institute for Infection and Immunity, 792 Elizabeth St, Victoria, 3000, Australia. [6]Present address: The Walter and Eliza Hall Institute of Medical Research, Parkville, Australia. [7]Present address: School of Life Sciences, Faculty of Science, University of Technology Sydney, Ultimo, Australia.
✉e-mail: preading@unimelb.edu.au

splice variant of hGBP3 (hGBP3ΔC) also inhibited IAV infectivity by blocking viral transcription and replication at the level of, or prior to, synthesis of viral mRNA[12]. Moreover, hGBP2 and hGBP5 were reported to suppress proteolytic processing of envelope glycoproteins from numerous viruses, including a highly pathogenic avian influenza (HPAI) H7N7 virus, human immunodeficiency virus (HIV)-1, MeV and ZIKV, by inhibiting the cellular protease furin[14]. A recent study reported that hGBP2 and hGBP5 also interfered with furin-mediated cleavage of the spike protein of SARS-CoV-2 to restrict early-lineage SARS-CoV-2 isolates but did not restrict the infectivity of Alpha and Delta variants of concern (VOCs)[15].

In contrast to the growing number of in vitro studies describing the antiviral properties of hGBPs, few have reported the ability of mouse (m) GBPs to inhibit different viruses in vitro or in vivo. This is surprising given that mGBP-deficient mice have been used extensively to define the importance of GBPs in immunity to different intracellular bacteria and protozoa (reviewed in ref. 7), but similar studies assessing their role in antiviral immunity are currently lacking. Of the in vitro studies published to date, Pan et al. demonstrated that silencing of mGBP1 in mouse macrophages was associated with a modest increase in titres of dengue virus (DENV) at 24 h post-infection[16]. Moreover, constitutive overexpression of mGBP2 in NIH 3T3 cells reduced titres of VSV and EMCV by ~48% and ~42%, respectively, with the GTP-binding motif of mGBP2 required for inhibition of EMCV but not for inhibition of VSV[17,18]. More recent studies demonstrated that mGBP2 is important for IFN-γ–dependent antiviral activity in mouse macrophages against murine norovirus (MNV)[19,20].

We recently reported that mGBP1 did not inhibit IAV replication in vitro or in a mouse model of IAV infection[21]. Given the increasing number of studies describing the antiviral activities of hGBPs against different viruses in vitro, we broadened our studies to investigate the antiviral activities of mGBPs of the chromosome 3 cluster (mGBPchr3, namely mGBP1/2/3/5/7) against IAV, herpes simplex virus (HSV)-1, Sendai virus (SeV), lymphocytic choriomeningitis virus (LCMV) and encephalomyocarditis virus (EMCV) in vitro. We did not detect significant differences in the growth of any of these viruses following overexpression of individual mGBPchr3 in mouse LA-4 cells, or in cells isolated from wild type (WT) and mGBPchr3 KO mice. Moreover, there were no significant differences in virus titres recovered from WT versus mGBPchr3 KO mice following intranasal, intraperitoneal or flank zosteriform infections with IAV, LCMV or HSV-1, respectively. Collectively, these data indicate that mGBPchr3 do not appear to be a major component of cell-intrinsic antiviral immunity, at least against any of the diverse viruses tested in our studies.

Results

Induction of chromosome 3 cluster mGBPs and generation of cell lines with DOX-inducible overexpression of individual FLAG-tagged mGBPs

To gain insight regarding constitutive expression of mGBPs and their induction following IAV infection, we analysed RNA-sequencing data from type II airway epithelial cells (ATII) and airway macrophages (AM) previously generated in our laboratory. In these studies[22], lungs were collected from mock- or IAV-infected wild-type C57BL/6 mice or C57BL/6 mice deficient in IRF3 and IRF7 (*Irf3/7*$^{-/-}$) at 10 hr post-infection (hpi) and ATII cells and AM purified by flow cytometry were subjected to RNA-sequencing. Given the availability of a knockout mouse deficient in chromosome 3 cluster mGBPs (mGBPchr3 KO mice), we focussed our analyses on mGBPs in the mGBPchr3 cluster, namely mGBP1/2/3/5/7. In ATII cells, mGBP2 and mGBP7 showed the highest levels of constitutive expression in WT mice and all mGBPchr3 were upregulated after IAV infection, although only modest IAV-induced upregulation was observed in *Irf3/7*$^{-/-}$ ATII (Fig. 1a). In AM, mGBP2 and mGBP7 were again expressed at the highest constitutive levels and again all mGBPchr3 were upregulated in response to IAV (Fig. 1b). Data are also represented as bar graphs with individual data points (Supplementary Fig. 1). Again, IAV-induced upregulation of individual mGBPchr3 was largely IRF3/7-dependent. Given that multiple mGBPchr3 are expressed in parenchymal (ATII) and immune (AM) cells of the lung and most are upregulated following IAV infection, we investigated the ability of each mGBPchr3 to mediate antiviral activity against IAV, or against additional human or mouse viruses.

To assess the ability of individual mGBPchr3 to mediate antiviral activity in vitro, we generated LA-4 cell lines (mouse type II airway epithelial-like cells) with stable doxycycline (DOX)-inducible overexpression of individual mGBPchr3, reasoning that expression of additional mouse proteins, including endogenous mGBPs and other ISGs, might be required for the effective function of overexpressed mGBPchr3 proteins. We used a lentiviral vector system to generate cells with DOX-inducible overexpression of individual FLAG-tagged mGBPchr3 proteins, noting that we have previously used this approach to demonstrate the antiviral activity of different host cell restriction factors[23–25], including the related GTPase mouse (m)Mx1 against IAV and HSV-1 in LA-4 cell lines[26]. Flow cytometric analyses confirmed expression of individual mGBPchr3 proteins in LA-4 cells following induction with DOX whereas LA-4-CTRL cells showed negligible FLAG expression in the presence or absence of DOX (Fig. 1b, gating strategy Supplementary Fig. 2).

Next, we used qRT-PCR to assess induction of individual mGBPchr3 in (i) LA-4-CTRL cells following stimulation with recombinant mouse IFN-α, as well as (ii) LA-4 cells with DOX-inducible overexpression of individual FLAG-tagged mGBPchr3 proteins. First, constitutive expression (i.e. the difference in Ct values of each mGBP relative to GAPDH ($2^{-\Delta Ct}$)[27]) of each mGBP in untreated LA-4-CTRL cells were determined (Supplementary Fig. 3). IFN-α treatment of LA-4-CTRL cells resulted in >100-fold upregulation of mGBP1, 2, 3 and 7, while mGBP5 was upregulated ~20-fold compared to mock-treated control cells (Fig. 1c(i)). Additional ISGs, namely Mx1 and ISG15, were also upregulated by IFN-α treatment as expected (Fig. 1c(ii)). When examining LA-4 cells with DOX-inducible expression of individual FLAG-tagged mGBPchr3, we noted ~100–200 fold induction of mGBP1, 2, 3 and 7 in each cell respective cell line following DOX treatment, with mGBP5 induced to more modest levels, ~50-fold higher than those of mock-treated cells (Fig. 1c(iii)). Of note, DOX treatment of LA-4-CTRL cells did not result in significant induction of any individual mGBPchr3, confirming that DOX treatment did not modulate expression of endogenous mGBP expression. Together, these data confirm that each individual mGBPchr3 is upregulated in LA-4-CTRL cells following treatment with IFN-α and that DOX-treatment induces induction of individual FLAG-tagged mGBPchr3 to similar levels to that of IFN-α.

DOX-inducible overexpression of individual mGBPchr3 proteins did not inhibit the ability of different human or mouse viruses to replicate in LA-4 cells in vitro

We next aimed to determine if mouse LA-4 cells with DOX-inducible expression of individual mGBPchr3 could inhibit growth of different viruses. For these studies, we have utilised human (IAV, HSV-1) and mouse viruses (SeV, LCMV and EMCV) from diverse virus families, namely *Orthomyxoviridae* (IAV), *Herpesviridae* (HSV-1), *Paramyxoviridae* (SeV), *Arenaviridae* (LCMV) and *Picornaviridae* (EMCV). Moreover, this virus panel includes viruses which replicate primarily in the nucleus (IAV, HSV-1) or in the cytoplasm (SeV, LCMV and EMCV). Preliminary experiments optimised virus growth in parental LA-4 cells in terms of multiplicities of infection (MOIs) and time points for peak virus growth, confirming a marked enhancement in virus titres between 2 h post-infection (hpi) and 24 hpi (IAV, EMCV) or 48 hpi (HSV-1, SeV, LCMV) following titration by ViroSpot (VS) or plaque assay (Fig. 2a).

Next, cell lines with inducible overexpression of individual mGBPchr3 were cultured in the presence (DOX) or absence (no DOX) of 1 μg/mL of DOX for 24 hr, infected with different viruses (MOI as shown) and virus growth was determined 24 hpi (IAV, EMCV) or 48 hpi (HSV-1, SeV, LCMV). While some variation was observed in titres of particular viruses recovered from different mGBPchr3 cell lines, for any one cell line cultured in the presence or absence of DOX we did not observe a significant reduction in titre of IAV (Fig. 2b), HSV-1 (Fig. 2c), SeV (Fig. 2d), LCMV (Fig. 2e) or EMCV (Fig. 2f). As a control for the

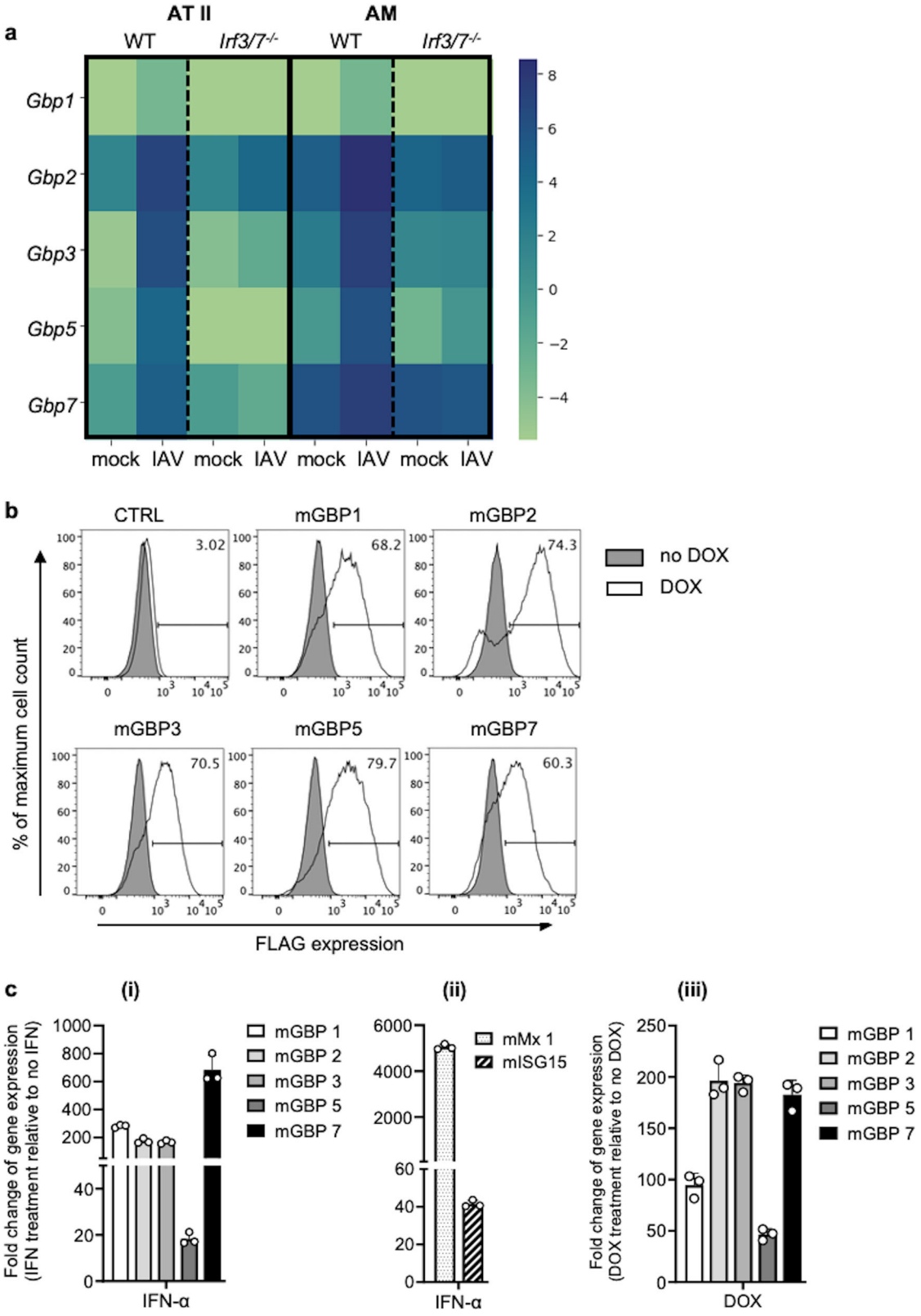

integrity of the DOX-inducible overexpression system in LA-4 cells, we confirmed that inducible expression of the related GTPase mouse (m) Mx1, also with a N-terminal FLAG tag), inhibited replication of IAV and HSV-1 (Fig. 2b, c), but not LCMV, SeV or EMCV (Fig. 2d–f). In addition to data shown using MOI = 1, none of the DOX-inducible mGBPs showed inhibition of IAV or HSV-1 at 24 or 48 hpi when lower MOI (0.1) was used (Supplementary Fig. 4). Together, these data indicate that inducible overexpression of each individual mGBPchr3 in LA-4 cells prior to infection did not impact subsequent growth of any of the five different viruses tested.

Fig. 1 | Expression of mGBPchr3 in cells isolated from IAV-infected mice and characterisation of cells with DOX-inducible expression of single mGBPchr3. **a** C57BL/6 (WT) mice and mice deficient in both IRF3 and IRF7 (*Irf3/7*$^{-/-}$) infected with 10^6 PFU of IAV (PR8, H1N1) or an equivalent volume of uninfected allantoic fluid (mock) were euthanised 10 hpi, and fluoroscent-labeled antibodies and cell sorting were used to isolate alveolar type II epithelial cells (ATII) and alveolar macrophages (AM), for RNA-seq as described in ref. 22. Data was aligned to the mouse transcriptome, aligned fragments were summarised into genes and raw counts were transformed to $\log_2$ counts per million. Normalization and differential expression testing were conducted using edgeR. Dark blue and light green correspond to high and low expression, respectively. For heatmaps, average $\log_2$ count per million of $n = 4$ independent biological replicates are shown. The heatmaps were generated using Plotly. The RNA-seq data available via NCBI GEO database: accession number GSE115904. **b** LA-4 cells with DOX-inducible expression of individual FLAG-tagged mGBP1/2/3/5/7 (or CTRL cells) were cultured for 24 h in media with (DOX) or without (no DOX) 1 μg/mL DOX. Cells were detached, fixed, permeabilised and stained for intracellular expression of FLAG-tagged protein before analysis by flow cytometry. Representative histograms of cells cultured in DOX (open) or no DOX (shaded) are shown. Data are representative of $n = 3$ independent experiments. **c** Induction of mouse GBP1/2/3/5/7 following IFN-α treatment of LA-4 CTRL cells or DOX treatment of LA-4 cells expressing individual DOX-inducible mGBPchr3. (**i**/**ii**) LA-4-CTRL were untreated or treated with 1000 mU/mL IFN-α and, after a further 24 h, cells were lysed for RNA extraction and qRT-PCR. (**i**) mGBPchr3, or (**ii**) mMx1 and ISG15 in response to IFN-α treatment. Results from IFN-α-treated samples were normalized to mouse GAPDH and then expressed as fold-change relative to untreated (no IFN). (**iii**) LA-4 cells with DOX-inducible expression of individual FLAG-tagged mGBPchr3 were treated with 1 μg/mL DOX and, after a further 24 h, cells were lysed for RNA extraction and qRT-PCR. Results from triplicate DOX-treated samples were normalized to mouse GAPDH and then expressed as fold-change relative to no DOX. Data show the mean ± SD expression of triplicate samples from 1 of 2 independent experiments.

DOX-inducible mGBPchr3 can mediate cell-intrinsic immunity to bacteria

It is well established that mGBPchr3 play an important role in cell-intrinsic immunity to vacuolar and cytosolic bacteria, as well as to protozoan pathogens. While mGBPs, including mGBPchr3, have been particularly well studied in mouse macrophages (reviewed in ref. 7), they have also been implicated in limiting intracellular infections in parenchymal cells[28]. Given that none of the DOX-inducible mGBPchr3 inhibited growth of IAV, HSV-1, LCMV, SeV or EMCV in LA-4 cells, we sought additional evidence to confirm the functionality of the overexpressed mGBPchr3. Therefore, we assessed the growth of intracellular *E. coli* in LA-4 cells lines with DOX-inducible overexpression of individual mGBPchr3. LA-4 cells were first incubated for 24 hr in the presence of DOX, then cultured an additional 24 hr with or without IFN-γ prior to inoculation with GFP-labelled *E. coli*. At various times thereafter, cells were treated with gentamicin to kill extracellular bacteria, washed and the burden of intracellular *E. coli* determined by microscopy. In the absence of IFN-γ priming, a modest but significant reduction in *E. coli* was observed in cells with DOX-inducible overexpression of mGBP5 at 8 hpi and mGBP2 and mGBP5 overexpression were associated with significant reductions in intracellular bacteria at 12 hpi (Fig. 3a). When cells were primed with IFN-γ prior to bacterial challenge, overexpression of either mGBP2 or mGBP5 was associated with significant reductions in *E. coli* at 4, 8 and 12 hpi and potency was markedly enhanced relative to cells not primed with IFN-γ (Fig. 3a).

To confirm the importance of DOX-inducible mGBP2 and mGBP5 in enhancing clearance of intracellular *E. coli*, LA-4 cells were cultured in the presence (DOX) or absence (no DOX) of DOX, cultured an additional 24 h with our without IFN-γ, inoculated with GFP-labelled *E. coli* and analysed at 8 hpi. In the absence of IFN-γ priming, DOX-inducible mGBP5, but not mGBP2, significantly reduced levels of intracellular bacteria (Fig. 3b). Moreover, the antibacterial effect of IFN-γ priming was markedly enhanced in the presence of DOX-induced mGBP2 and mGBP5 (Fig. 3b). Thus, consistent with previous reports that mGBP2 and mGBP5 promote clearance of intracellular bacteria[1,29–31], these results confirm the functionality of the overexpressed mGBPchr3 proteins in LA-4 cells.

Human and mouse viruses replicate to similar levels following infection of mouse lung fibroblasts isolated from mice which do or do not express the mGBPchr3 cluster, irrespective of pre-treatment with IFN

DOX-inducible overexpression of individual mGBPchr3, namely mGBP1/2/3/5/7, in mouse LA-4 cells did not have a major impact on the growth of IAV, HSV-1, SeV, LCMV or EMCV in vitro (Fig. 2b–f). However, given that different mGBPchr3 have been reported to act cooperatively in mediating antibacterial and antiprotozoal activities (reviewed in refs. 1,7), we hypothesised that overexpression of any individual mGBP may not be optimal for potent antiviral activity. Therefore, we next aimed to assess virus replication in cells from wild-type (WT) mice as well as in mice lacking the entire mGBPchr3 cluster (mGBPchr3 KO)[32]). Preliminary experiments optimised virus growth in mouse lung fibroblasts (MLFs) using different MOIs and time points for peak virus growth, confirming a marked enhancement in virus titres between 2 and 24 hpi (IAV, EMCV) or 48 hpi (HSV-1, SeV, LCMV) following titration by ViroSpot (VS) or plaque assay (Fig. 4a). To assess mGBPchr3 expression, we first determined constitutive expression of each mGBPchr3 in untreated MLF (Supplementary Fig. 3). Furthermore, we confirmed upregulation of individual mGBPchr3 in WT MLF in response to 1000 U/mL of mouse IFN-α or 20 mU/mL of IFN-γ, noting that induction of mGBP1 was relatively low (0–10 fold) in response to both stimuli (Fig. 4b(i)). While mGBPchr3 mRNA is not expressed in cells from mGBP chr3 KO mice[32], analysis of Mx1 and ISG15 induction confirmed no significant differences in induction of other ISG in WT versus mGBPchr3 KO MLF, noting that overall levels of induction were lower in IFN-γ-treated compared to IFN-α-treated cells (Fig. 4b(ii)).

Next, virus growth was determined in MLFs from mGBPchr3 KO cultured in the presence or absence of pre-treatment with IFN-γ prior to infection. Therefore, cell monolayers were cultured overnight in media alone (no IFN) or media supplemented with 20 mU/mL of IFN-γ (IFN-γ), then infected with IAV (MOI = 10), HSV-1 (MOI = 1), SeV (MOI = 1), LCMV (MOI = 0.5) and EMCV (MOI = 0.1) and supernatants removed at 2 hpi (residual inoculum) or 24/48 hpi (virus growth) were clarified and titres of infectious virus determined. In media alone, no significant differences were noted in virus titres recovered from WT or mGBPchr3 KO MLFs (Fig. 4c). Pre-treatment of cells with IFN-γ reduced virus titres at 24/48 hpi when compared to untreated cells, however we did not detect any significant differences in virus growth in IFN-γ-treated MLFs derived from WT or mGBPchr3 KO mice (Fig. 4c). Similarly, we did not observe differences in the growth of any virus tested in MLFs from WT or mGBPchr3 KO mice following pre-treatment with 100mU/mL of IFN-γ.

Given the importance of type I IFNs in the context of viral infections, we next pre-treated MLF from WT or mGBPchr3 KO mice with 1000 U/mL of recombinant mouse IFN-α (IFN-α), then infected with different viruses (MOI indicated), and assessed virus growth. As expected, pre-treatment of cells with IFN-α resulted in reduced virus titres at 24/48 hpi when compared to untreated (no IFN) cells (Fig. 4d). Again, we did not detect any significant differences in virus growth between IFN-α-treated MLFs derived from WT or mGBPchr3 KO mice (Fig. 4d). Given the potent inhibition of virus growth observed following pre-treatment with mouse IFN-α, we also confirmed no difference in growth of any virus between IFN-α-treated MLFs derived from WT or mGBPchr3 KO mice following infection with a higher MOI for IAV (MOI = 50), HSV-1 (MOI = 10), SeV (MOI = 10), LCMV (MOI = 5) and EMCV (MOI = 1). Overall, these data show that while MLFs support growth of IAV, HSV-1, EMCV, LCMV and SeV, no differences were detected in the growth of any virus in cells which do or do not express mGBPchr3. This was true even if cells were pre-treated with IFN-γ or IFN-α to upregulate expression of mGBPs and other ISGs prior to virus infection.

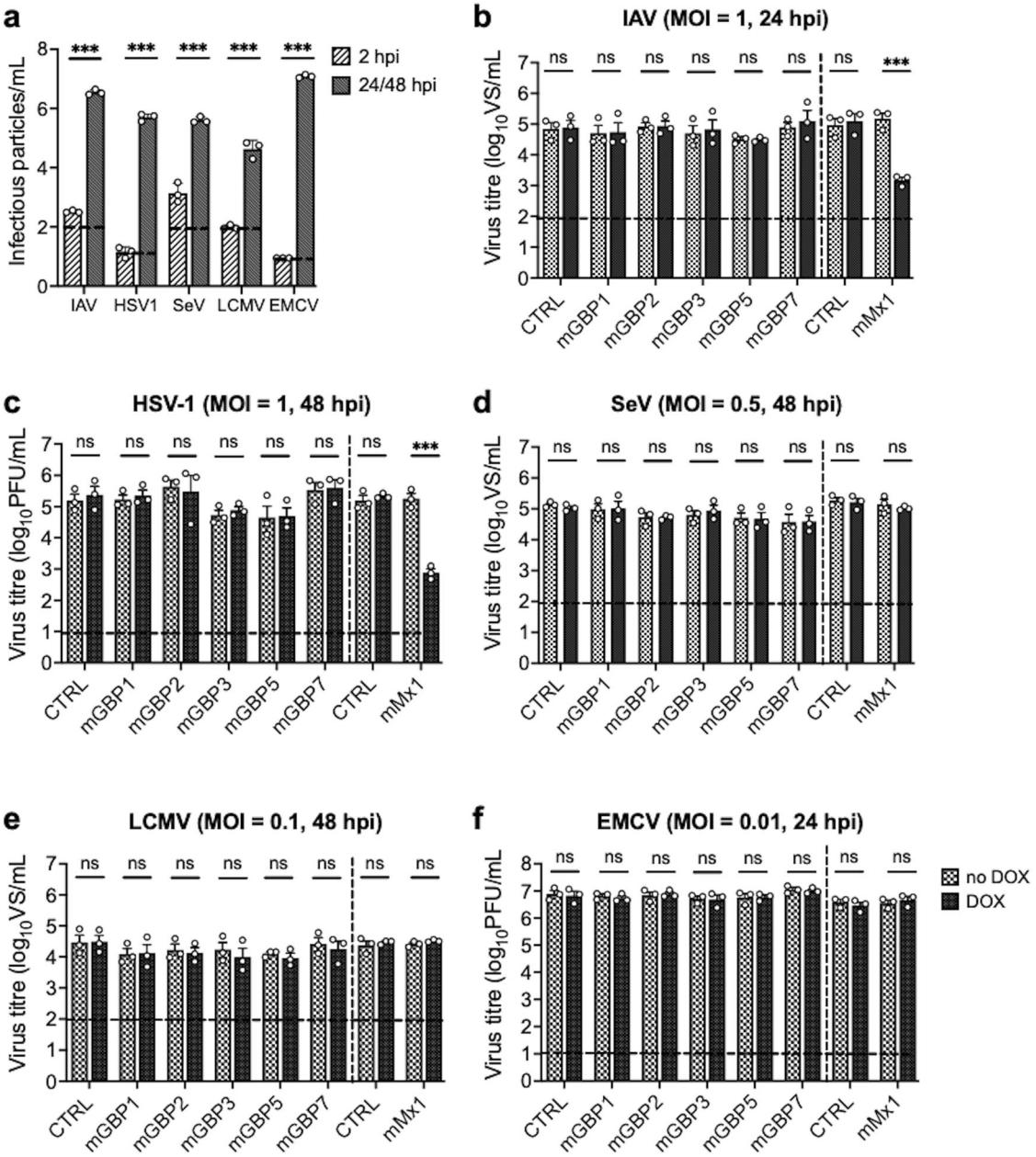

Fig. 2 | DOX-inducible expression of mGBP1/2/3/5/7 in LA-4 cells does not modulate growth of IAV, HSV-1, SeV, LCMV or EMCV. a Parental LA-4 cells were cultured overnight and infected with IAV, SeV or HSV-1 (MOI = 1), or with LCMV or EMCV (MOI = 0.1) for 60 min at 37 °C, washed and cultured at 37 °C. At 2 hpi and 24 hpi (IAV and EMCV) or 48 hpi (SeV, HSV-1, LCMV), supernatants were removed, clarified and virus titres determined by VS assay (IAV, SeV, LCMV) or plaque assay (HSV-1, EMCV). Data show the mean ± SD of triplicate samples. **b**–**f** LA-4 cells with DOX-inducible expression of mGBP1/2/3/5/7, as well as CTRL and mMx1 cells, were cultured overnight and media was then supplemented with (DOX) or without (no DOX) 1 μg/mL DOX for 24 hr. After DOX induction, cells were incubated with IAV (**b**), HSV-1 (**c**), SeV (**d**), LCMV (**e**) and EMCV (**f**) at the indicated MOI for 1 h at 37 °C, washed and returned to culture. At 24 hpi (IAV and EMCV) or 48 hpi (SeV, LCMV and HSV-1), supernatants were removed, clarified and titres of infectious virus determined by plaque or VS assay. Data show the mean ± SE from 3 independent experiments, each with triplicate samples. The horizontal dashed line represents the detection limit of the VS or plaque assay. Statistical significance was determined by Student's t-test; *** $p < 0.001$; ns not significant.

While no major changes in virus growth were detected between MLF from WT or mGBPchr3 KO mice, it is possible that mGBPchr3 could modulate other virus-induced responses, such as virus-induced cytokine and chemokine production. Therefore, we used the BD™ cytometric bead array (CBA) mouse anti-virus response panel kit to examine inflammatory mediators released from WT or mGBPchr3 KO MLFs under the same experimental conditions as those used to assess virus growth. We determined the levels of IFN-γ, CXCL1, TNF-α, CCL2, IL-12, CCL5, IL-1β, CXCL10, GM-CSF, IL-10, IFN-β, IFN-α and IL-6 in cell-free supernatants harvested from virus-infected cells. These studies include analysis of supernatants from cells cultured in media alone (no IFN) or pre-treated with 1000 U/mL of recombinant mouse IFN-α (IFN-α) prior to infection. Data are presented as the fold change of each mediator relative to mock-infected cells (Fig. 4e). A number of conclusions can be drawn from this data. First, it is clear that each virus infection induced a unique spectrum of inflammatory mediators from MLF. Viruses such as HSV-1, SeV and LCMV induced similar patterns of inflammatory mediators when compared to IAV and EMCV, which each induced a very distinct spectrum. Such differences likely relate to virus-specific properties, including the particular pattern recognition receptors (PRRs) triggered and specific immune antagonists encoded

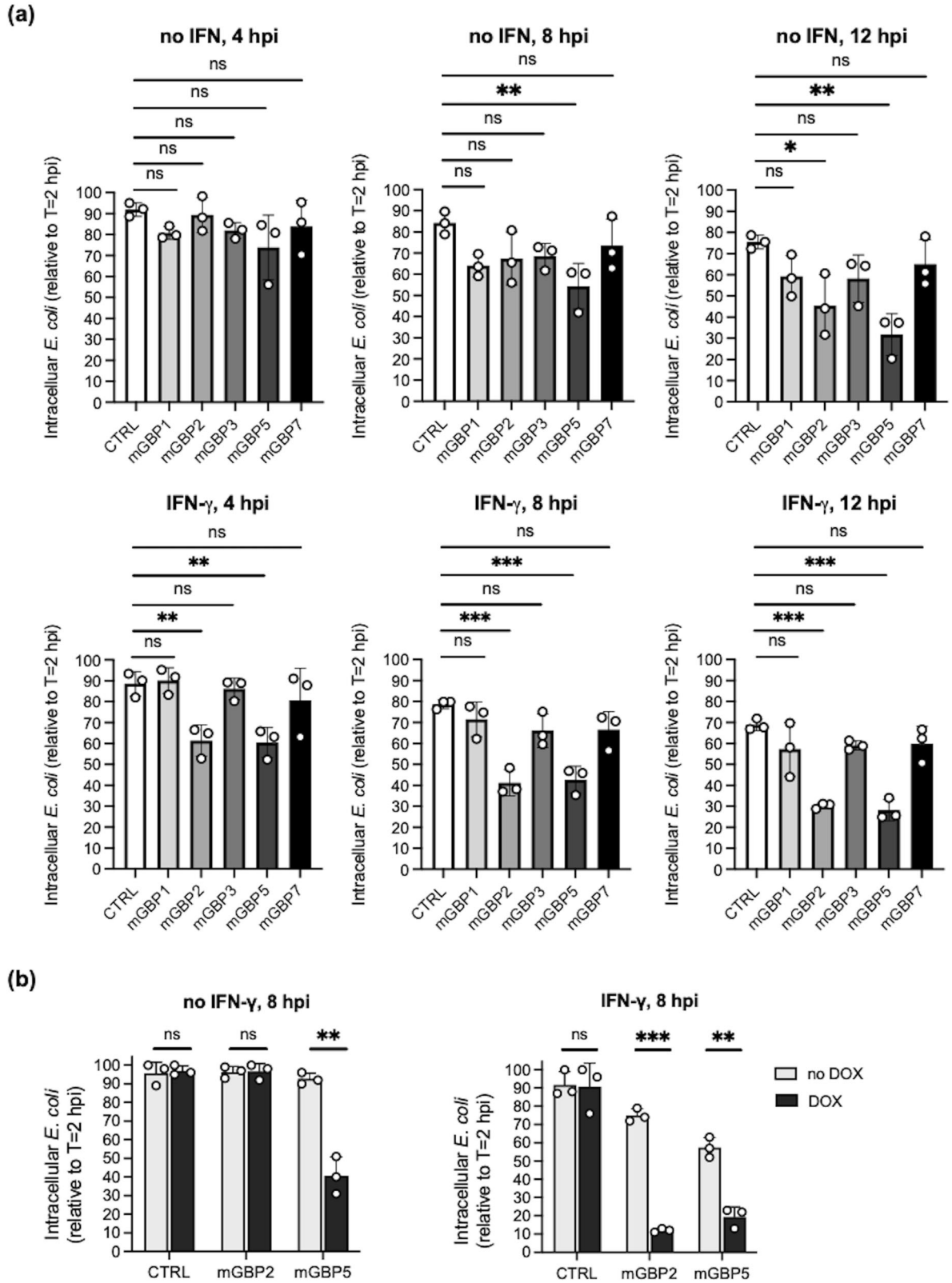

Fig. 3 | Overexpression of individual DOX-inducible mGBPchr3 in LA-4 cells results in antibacterial activity. LA-4 cells with DOX-inducible overexpression of mGBP1/2/3/5/7, as well as CTRL cells, were seeded and incubated overnight. **a** Media was then supplemented with 1 µg/mL DOX. After overnight culture, cells were left untreated or treated with 100 U/mL of mouse IFN-γ for 24 h before they were infected with GFP-*E. coli* (MOI 20). At 4, 8 and 12 hpi cells were monitored using the IncuCyte Zoom imaging system (Essen Biosciences) to track the number of intracellular GFP-*E. coli* over time. **b** A similar experiment was performed, but this time cells were cultured overnight with (DOX) or without (no DOX) 1 µg/mL DOX and then left untreated (no IFN-γ) or treated with 100 U/mL of mouse IFN-γ for 24 h (IFN-γ), then infected with GFP-*E. coli* (MOI 20) and analysed at 8 hpi. Data show the mean ± SE from 3 independent experiments, each with triplicate samples. Statistical significance was determined by (**a**) one way ANOVA (**b**) by Student's t-test; * $p < 0.05$; ** $p < 0.01$; *** $p < 0.001$; ns not significant.

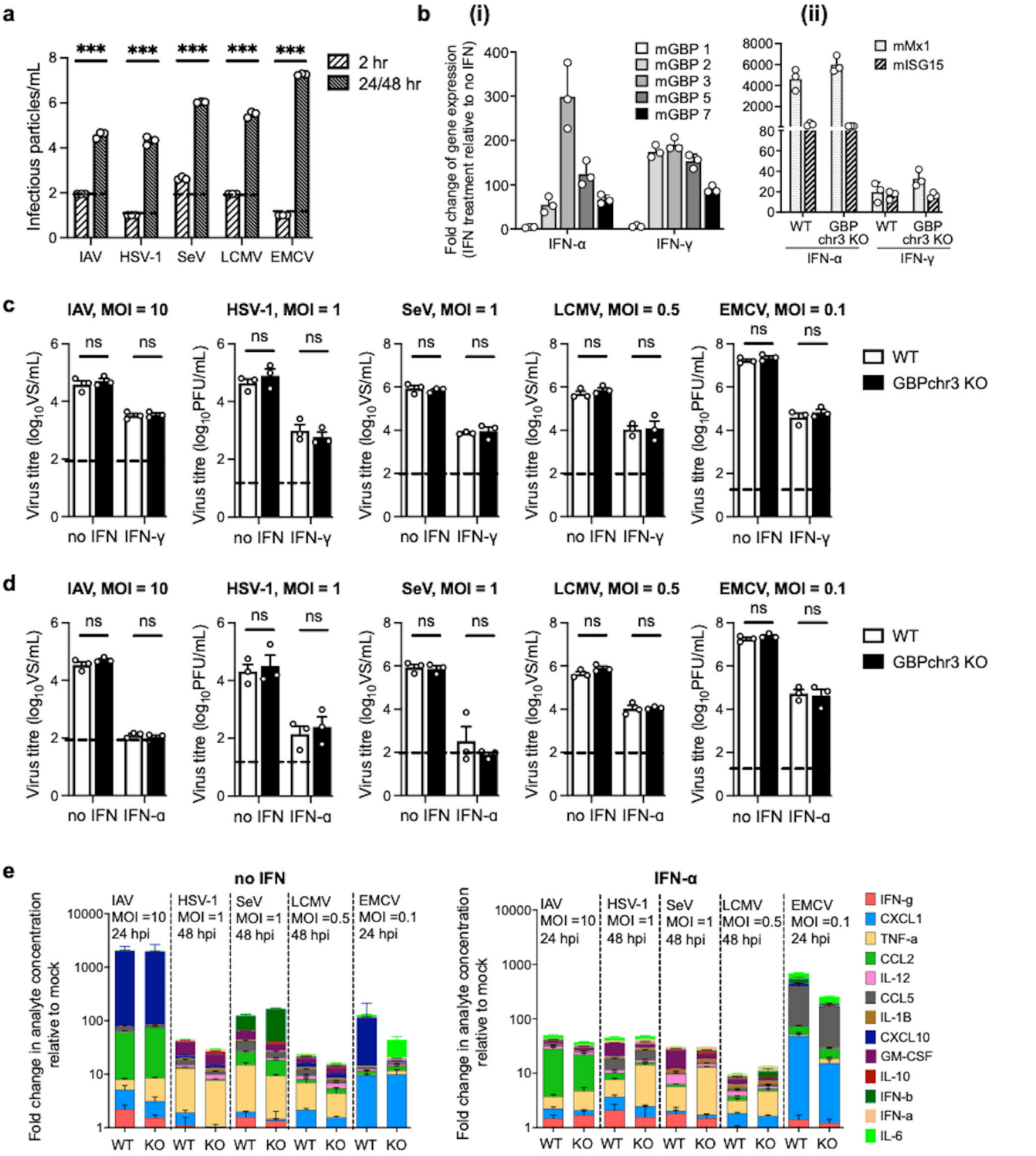

Fig. 4 | Primary lung fibroblasts from WT or mGBPchr3 KO mice support similar levels of growth following infection by different human and mouse viruses in vitro. Mouse lung fibroblasts (MLF) from WT and mGBPchr3 KO mice were cultured overnight. The next day, cells were incubated with (**b**, **c**) 20 U/mL IFN-γ, or (**b**, **d**, **e**) 1000 U/mL IFN-α (IFN-α), or with media alone (no IFN) for 24 h. **b** Cells were lysed for RNA extraction and qRT-PCR. (**i**) mGBPchr3, or (**ii**) mMx1 and ISG15 in response to IFN-α treatment. Results from IFN-treated samples were normalized to mouse GAPDH and then expressed as fold-change relative to no IFN. Data show the mean ± SE expression of triplicate samples from 1 of 2 independent experiments. **a**, **c**, **d** Cells were infected with IAV, HSV-1, SeV, LCMV or EMCV at the indicated MOI. **a** At 2 hpi and 24 hpi (IAV and EMCV) or 48 hpi (HSV-1, SeV and LCMV), (**c**,**d**) At 24 hpi (IAV and EMCV) or 48 hpi (HSV-1, SeV and LCMV), supernatants were removed, clarified and titres of infectious virus were determined by VS assay on MDCK (IAV) or HEp-2 cells (SeV and LCMV), or by plaque assay on Vero cells (HSV-1 and EMCV). Data show the mean ± SE from (**a**) 1 of 2 independent experiments. **c**, **d** 3 independent experiments, each with triplicate samples. The dashed line represents the detection limit of the VS or plaque assay. Statistical significance was determined by Student's t-test; ns not significant. **e** At 24 hpi (IAV and EMCV) or 48 hpi (HSV-1, SeV and LCMV), supernatants were removed, clarified and analysed by flow cytometry using a multiplex CBA assay to detect 13 different inflammatory cytokines and chemokines. Fold change in concentration of each analyte was calculated relative to supernatants from mock-infected cells. Data show the mean ± SE of data from 2 independent experiments performed in triplicate.

by particular viruses, as well as differences in infection efficiency and kinetics of virus replication. Second, pre-treatment with IFN-α induced changes in the repertoire and magnitude of induction of specific inflammatory mediators for some of the viruses tested. For example, while IFN-α pre-treatment enhanced production of some cytokines and chemokines in EMCV-infected MLFs (e.g., favouring a switch from CXCL10 to CCL5 production), the overall induction is diminished when compared to MLFs pre-treated with IFN-α and then infected with IAV, HSV-1, SeV or LCMV. An important consideration here may relate to the susceptibility of MLFs to infection by each virus following IFN-α pre-treatment, given that titres of virus released from IFN-treated infected cells were markedly reduced compared to untreated cells (Fig. 4e).

Of note, the overall patterns of induction observed with each virus were very similar following infection of MLFs from WT and mGBPchr3 KO mice. When examining the fold change of each of the 13 individual mediators in response to each virus, we observed significant differences in some cytokines or chemokines induced in WT compared to mGBPchr3 KO cells (Supplementary Fig. 5). Despite these differences, overall we conclude that there were no major defects in the spectrum or the levels of inflammatory mediators produced by mGBPchr3 KO cells in response to different virus infections presented in this study.

Human and mouse viruses replicate to similar levels in mouse BMDM isolated from mice which do or do not express the mGBPchr3 cluster, irrespective of pre-treatment with IFN

Given that immune cells, including macrophages, can also modulate host defence during viral infections we next examined the ability of different viruses to replicate productively in BMDM from WT and mGBPchr3 KO mice. First, we investigated growth of different viruses in BMDM from WT mice at 2 versus 24/48 hpi. While all viruses tested showed productive replication in MLF, results were more variable following infection of BMDMs. Consistent with previous reports, IAV[33] and HSV-1[34], showed little evidence of growth in BMDMs (compare titres at 2 versus 24/48 hpi) (Fig. 5a), whereas mouse viruses (SeV, LCMV and EMCV) all showed evidence of significant virus growth (Fig. 5a). Next, we confirmed (i) consititutive expression (Fig. 5b(i)) and induction of each individual mGBPchr3 in WT BMDM in response to treatment with 1000 mU/mL of IFN-α (Fig. 5b(ii)), and (ii) that BMDM from WT versus mGBPchr3 KO mice produced equivalent levels of other ISGs, namely Mx1 and ISG15, in response to treatment (Fig. 5b(ii)).

BMDM from WT or mGBPchr3 KO mice were cultured in media alone or pre-treated with 1000 mU/mL of IFN-α and then infected with different viruses. For IAV and HSV-1 (Fig. 5c, d), WT and mGBPchr3 KO BMDM showed no differences in their ability to support virus growth and any modest viral growth was abrogated by pre-treatment of cells with IFN-α. Growth of SeV (Fig. 5e), LCMV (Fig. 5f) and ECMV (Fig. 5g) was equivalent in untreated BMDM from WT or mGBPchr3 KO mice and growth of each was abolished by pre-treatment with IFN-α. We note that under these experimental conditions it is possible that any effect mediated specifically by mGBPchr3 could be masked by the antiviral activities of other ISGs upregulated following IFN treatment. Overall, we did not observe any significant differences in virus titres following infection of BMDM isolated from WT or mGBPchr3 KO mice with human (IAV, HSV-1) or mouse viruses (EMCV, SeV, LCMV) in the presence or absence of pre-treatment with IFN-α.

To confirm the functionality of endogenous mGBPchr3, BMDMs from WT and mGBPchr3 KO mice, as well as mice lacking the type I IFN receptor (*Ifnar1*$^{-/-}$), were incubated with *E. coli* and, at 7 hpi or 15 hpi, incubated with geneticin for 1 hr to kill extracellular bacteria. After washing, BMDMs were lysed and plated to enumerate viable intracellular bacteria. Compared to WT BMDMs, significantly higher numbers of intracellular *E. coli* were recovered from mGBPchr3 KO and *Ifnar1*$^{-/-}$ BMDM at both 8 and 16 hpi (Fig. 5h). Thus, while we detected no differences in the growth of different viruses in cells from WT and mGBPchr3 KO mice in vitro, these data confirm the integrity of the WT and mGBPchr3 KO mouse lines used in our studies.

IAV-induced inflammasome activation in murine BMDM is not dependent on mGBPchr3 proteins

BMDM from mGBPchr3 KO mice show impaired inflammasome activation in response to a variety of intracellular bacteria ((reviewed in[35]). To determine whether the mGBPchr3 cluster plays a role during IAV-induced NLRP3 inflammasome activation, BMDMs from WT, mGBPchr3 KO mice or *Nlrp3*$^{-/-}$ mice[36] were infected with IAV strain HKx31 (MOI 25) before subsequent analysis of inflammasome activation at 12 hpi. As seen in Fig. 6, immunoblot analysis indicated that IAV infection induced caspase-1 activation, as indicated by the presence of the active caspase-1 p20 subunit, as well as the active p30 subunit of the pro-pyroptosis effector protein gasdermin D (GSDMD), in lysates from IAV-infected, but not mock-infected BMDMs (Fig. 6a, original blots shown in Supplementary Fig. 6). While evident in lysates from IAV-infected BMDMs from WT and mGBPchr3 KO mice, negligible caspase-1 p20 and GSDMD p30 were detected in BMDM lysates from *Nlrp3*$^{-/-}$ mice. Moreover, IAV infection induced similar levels of IL-1β and IL-18 in supernatants from WT and mGBPchr3 KO BMDMs, but levels were significantly lower in supernatants from IAV-infected *Nlrp3*$^{-/-}$ BMDMs (Fig. 6b). By comparison, LDH release was unaltered between IAV-infected WT, mGBPchr3 KO and *Nlrp3*$^{-/-}$ BMDMs and cells from WT, mGBPchr3 KO and *Nlrp3*$^{-/-}$ mice induced similar levels of TNF-α in response to IAV infection (Fig. 6b). In addition, there was no difference between WT and mGBPchr3 KO BMDMs following activation of the NLRP3 inflammasome by the canonical NLRP3 activator, adenosine triphosphate (ATP) (Fig. 6a). Overall, these data indicate that the entire cluster of mGBPchr3 is dispensable for IAV-mediated activation of the NLRP3 inflammasome.

mGBPchr3-deficient mice show no major differences in susceptibility to intranasal infection with IAV, flank infection with HSV-1 or intraperitoneal infection with LCMV

While the individual (overexpression) or collective (mGBPchr3 KO) effects of mGBPchr3 do not modulate the viruses tested in our in vitro studies, it is still possible that mGBPchr3 may impact other aspects of viral disease to modulate pathogenesis in vivo. Therefore, WT and mGBPchr3 KO mice were infected via the intranasal route with IAV and assessed for virus replication and airway inflammation at early and later time-points. At 3 or 7 days post-infection (dpi), mice were euthanised, and virus titres determined in homogenates prepared from the nose and lungs, or from cell-free bronchoalveolar lavage (BAL). As seen in Fig. 7a, high titres of virus were present in nasal tissues and lungs at 3 dpi, however no significant differences were noted between samples from WT or mGBPchr3 KO mice. By 7 dpi, virus titres were markedly reduced in nose, lungs and BAL samples and, again, no significant differences were observed between samples from WT or mGBPchr3 KO mice (Fig. 7a). Flow cytometry confirmed a higher neutrophil number in BAL from mGBPchr3 KO mice at 3 dpi (WT = $3.0 \times 10^5 \pm 1.3 \times 10^5$ versus mGBPchr3 KO = $5.5 \times 10^5 \pm 1.5 \times 10^5$, $p = 0.002$), but no other significant differences were recorded between mouse strains at either 3 or 7 dpi, including in numbers of pan-macrophages, alveolar macrophages, neutrophils, DC, NK cells or eosinophils. Numbers of T cells, particularly $CD8^+$ T cells, were low at 3 dpi (WT = $2.6 \times 10^3 \pm 1.9 \times 10^5$ versus mGBPchr3 KO = $1.6 \times 10^3 \pm 1.5 \times 10^3$, $p = 0.247$), but increased markedly at 7 dpi (WT = $2.3 \times 10^5 \pm 1.3 \times 10^5$ versus mGBPchr3 KO = $2.9 \times 10^5 \pm 1.9 \times 10^5$, $p = 0.449$), although no significant differences were noted.

Next, we performed flank skin zosteriform infections of WT and mGBPchr3 KO mice with HSV-1. Previous studies from our group have confirmed that virus replication can be detected as early as 3 dpi in both the primary (i.e., site of inoculation) and secondary skin sites (i.e., site of zosteriform lesions along entire dermatome), as well as the dorsal root ganglia (DRG), with peak titres recorded in all sites at 5 dpi[37]. Therefore, mice were euthanised at either 3 or 5 dpi and virus titres determined at each of the three sites. As seen in Fig. 7b, virus was recovered from the primary inoculation site and secondary skin lesions, as well as the DRG, of all infected animals

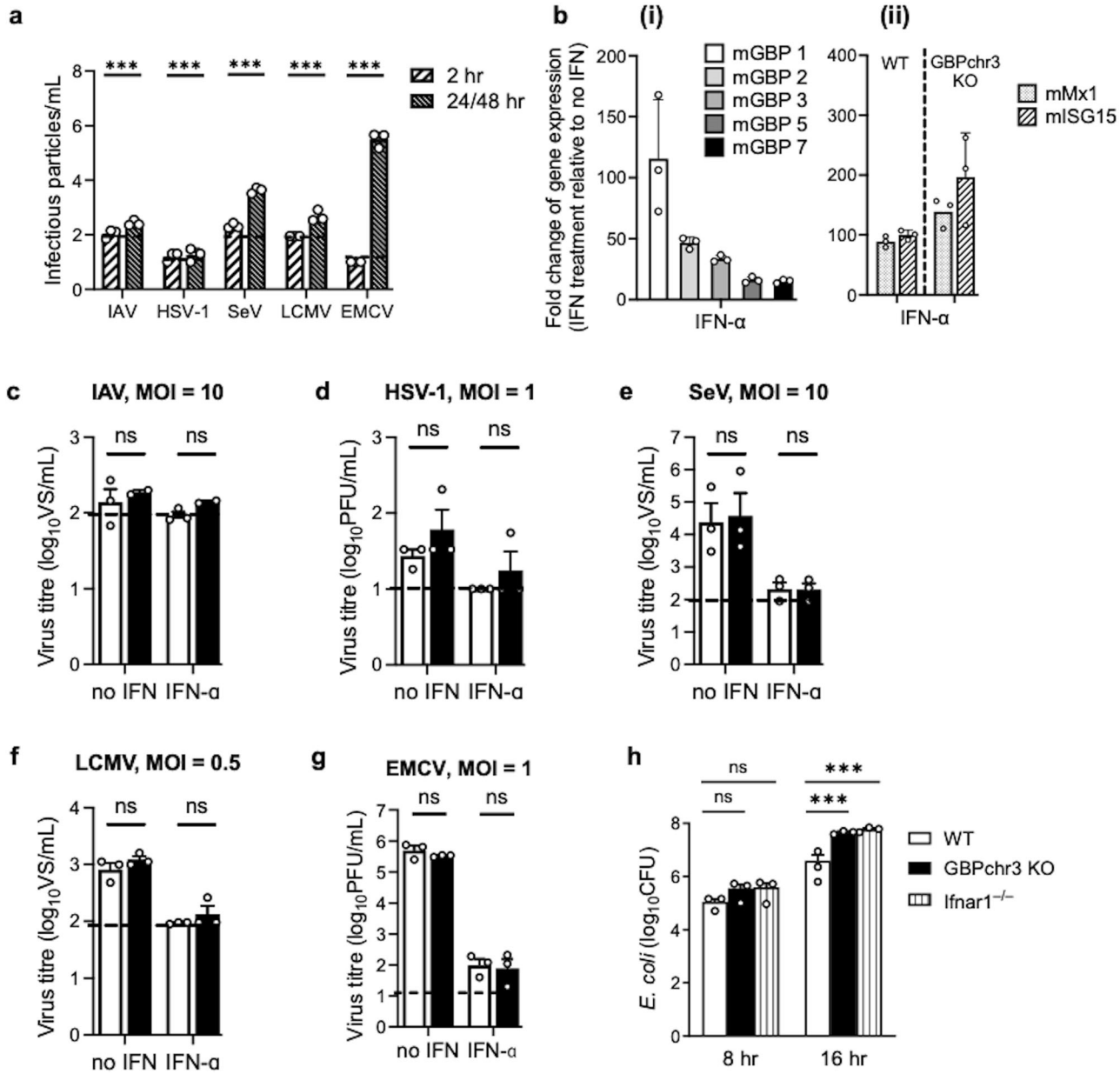

Fig. 5 | Human and mouse viruses show similar growth in BMDMs from WT or mGBPchr3 KO mice whereas mGBPchr3 KO BMDM support higher levels of bacterial growth. a Primary BMDMs from WT mice were cultured overnight. The next day, cells were infected with IAV (MOI = 10), SeV (MOI = 1), HSV-1 (MOI = 1), LCMV (MOI = 0.5) or with EMCV (MOI = 0.1) for 60 min at 37 °C, washed and cultured at 37 °C. At 2 hpi and 24 hpi (IAV and EMCV) or 48 hpi (SeV, HSV-1, LCMV), supernatants were removed, clarified and virus titres determined by VS assay (IAV, SeV, LCMV) or plaque assay (HSV-1, EMCV). Data show the mean ± SD of triplicate samples of 1 of the 2 independent experiments. **b** BMDM from WT and mGBPchr3 KO mice were incubated overnight and then treated with (IFN-α) or without (no IFN) 1000 U/mL of recombinant mouse IFN-α for 24 h. At 24 h post IFN-α treatment, cells were lysed for RNA extraction and qRT-PCR. (**i**) mGBPchr3, or (**ii**) mMx1 and ISG15 in response to IFN-α treatment. Results from IFN-treated samples were normalized to mouse GAPDH and then expressed as fold-change relative to no IFN. Data show the mean ± SD expression of triplicate samples. **c**–**g** BMDM from WT and mGBPchr3 KO mice incubated with (IFN-α) or without (no IFN) 1000 U/mL IFN-α for 24 h and then infected with (**c**) IAV, (**d**) HSV-1, (**e**) SeV, (**f**) LCMV or (**g**) EMCV at the indicated MOI. Supernatants were removed at 24 hpi (IAV and EMCV) or 48 hpi (HSV-1, SeV and LCMV) and titres of infectious virus determined. Data show the mean ± SE from $n = 3$ independent experiments. (**h**) BMDMs isolated from WT or mGBPchr3 KO mice were seeded and incubated overnight. The following day, cells were infected with *E. coli* (MOI 50). At 8 hpi and 16 hpi, cell lysates were serially diluted and plated onto LB agar to enumerate viable intracellular *E. coli*. Data show the mean ± SE from $n = 3$ independent experiments. **a**, **c**, **d**, **e**, **f**, **g**) The dashed line represents the detection limit of the VS or plaque assay. Statistical significance was determined by (**a**, **c**, **d**, **e**, **f**, **g**) Student's t-test or (**h**) two way ANOVA; *** $p < 0.001$; ns not significant.

however no significant differences in titres between WT and mGBPchr3 KO mice were noted at any site.

We also assessed the pathogenesis of LCMV (Armstrong) which is associated with an acute self-limiting infection in immunocompetent mice and intraperitoneal inoculation results in virus replication in a number of organs, including the kidney and spleen, and virus is generally cleared from organs by 7 dpi[38]. At day 3 after intraperitoneal injection with LCMV, virus was detected in clarified homogenates prepared from spleen and kidney, but no statistically significant differences were observed in virus titres between WT and mGBPchr3 KO mice (Fig. 7c). LCMV was not detected in the blood of any WT or mGBPchr3 KO mice at this time.

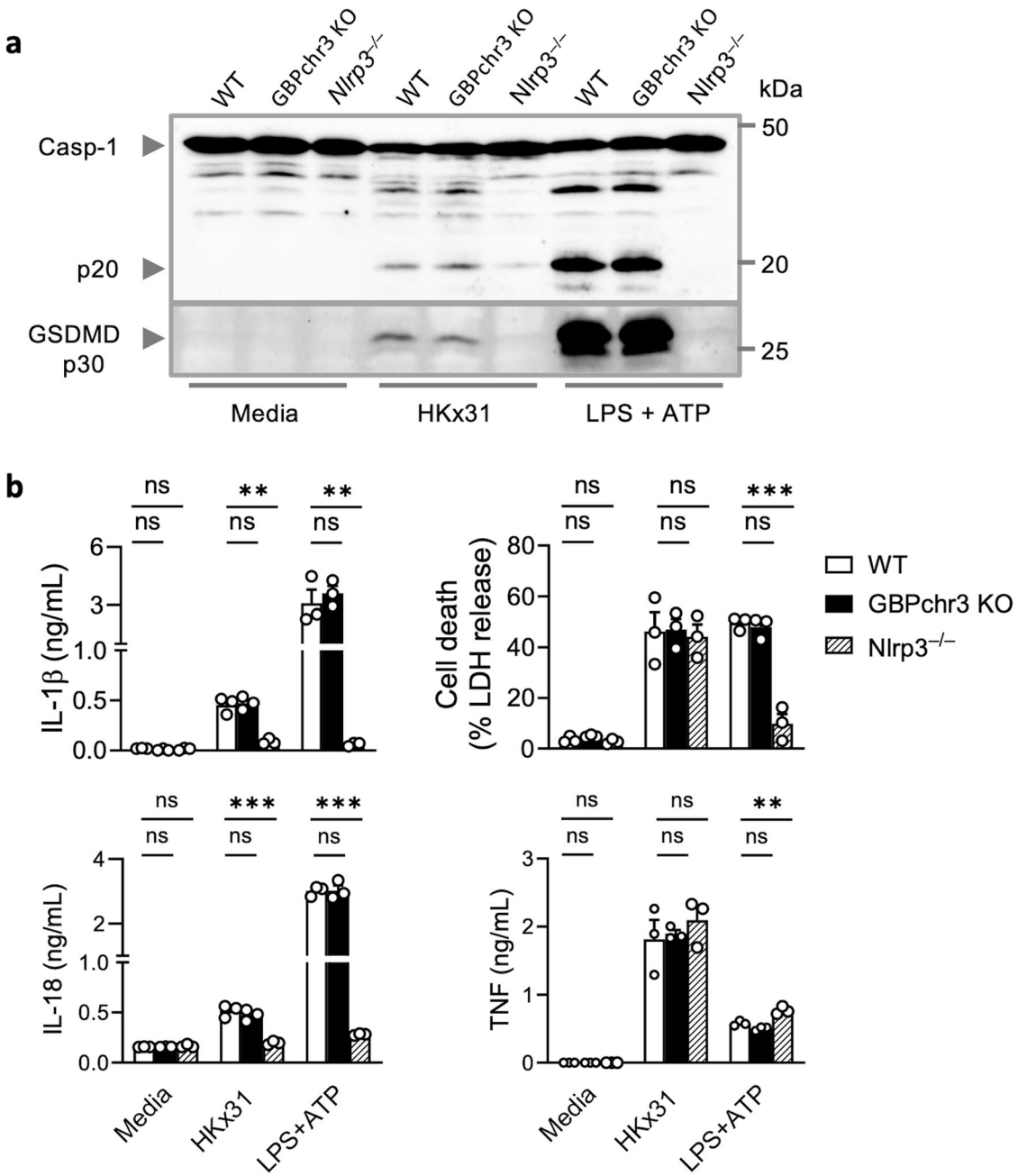

Fig. 6 | The mGBPchr3 cluster is dispensable for IAV-induced inflammasome activation in BMDMs in vitro. Primary BMDMs derived from WT, mGBPchr3 KO and *Nlrp3*$^{-/-}$ mice were mock-infected in serum-free media (Media) or infected with IAV strain HKx31(HKx31, MOI 25) for 16 hr or primed with 500 ng/mL ultrapure LPS from *E. coli* for 3 hr and then stimulated with 5 mM ATP for 45 min (LPS + ATP). **a** Cell lysates were collected for immunoblot analysis of pro-casapse-1 (Casp-1) and the active caspase-1 p20 subunit, pro-pyroptosis effector protein gasdermin D (GSDMD) and the active GSDMD p30 subunit. Original blots are shown in Supplementary Fig. 6. **b** Cell culture supernatants were collected to determine levels of IL-1β, IL-18, TNF and LDH. Data show the mean ± SE from 3 independent experiments, each with triplicate samples. Statistical significance was determined by Student's *t*-test; $^{**}p < 0.01$; $^{***}p < 0.001$; ns not significant.

Discussion

GBPs are potently induced by type II IFNs and it is well established that GBPs play a significant role in immunity to intracellular bacteria and protozoa both in vitro and in vivo in mouse models of infection[2,7,39–45]. Our initial studies confirmed upregulation of multiple mGBPchr3 in ATII and AM isolated from IAV-infected mice (Fig. 1), noting that most showed relatively modest upregulation in cells from IAV-infected *Irf3/7*$^{-/-}$ mice. Given the strong upregulation of mGBPchr3 during IAV infection, we hypothesised that one or more may play an important role in modulating IAV infection. Moreover, given relatively few studies have reported an antiviral role for mGBPs, we also aimed to assess their antiviral activity against a range of human and murine viruses both in vitro and in vivo. While different nomenclatures for *Mus musculus* GBPs have been proposed[46,47], the currently accepted nomenclatures[48,49] have been used throughout to avoid confusion.

Our in vitro studies utilized complementary approaches, namely (i) LA-4 cells with DOX-inducible overexpression of each individual mGBPchr3, and (ii) primary MLFs and BMDMs from WT versus mGBPchr3 KO mice to assess the impact of individual mGBP overexpression or the collective effect of endogenous mGBPchr3 proteins,

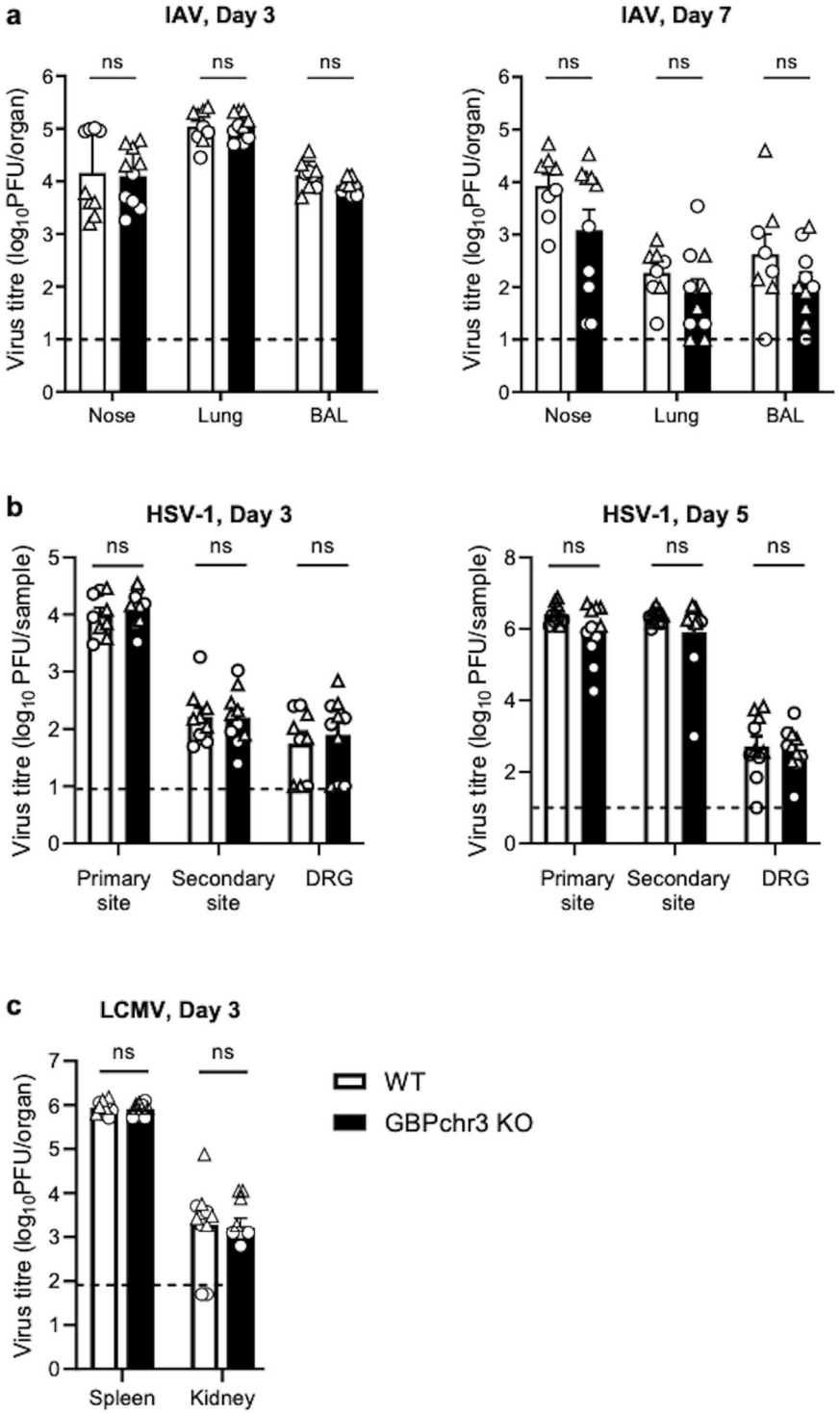

Fig. 7 | No differences in viral titres recovered following infection of WT or mGBPchr3 KO mice with IAV, HSV-1 or LCMV. a WT and mGBPchr3 KO mice were infected via the intranasal route with 50 µL of PBS containing 10^4 PFU of IAV strain HKx31 and at 3 (left) or 7 (right) dpi, mice were euthanised and virus titres in homogenates prepared from nasal tissues and lungs were determined by plaque assay on MDCK cells. **b** Mice were infected via flank scarification with 10^6 PFU of HSV-1 strain KOS and at 3 (left) and 5 (right) dpi, animals were euthanised and skin samples (corresponding to the primary and secondary sites) and the DRG were removed, and titres of infectious virus in clarified homogenates were determined by plaque assay on Vero cells. **c** Mice were infected via the intraperitoneal route with 50 µL of PBS containing 10^6 PFU of LCMV strain Armstrong and at 3 dpi, mice were euthanised and virus titres in homogenates of the spleen and kidney were determined by plaque assay on Vero cells. For (**a**–**c**), data show the mean ± SE and are pooled from $n = 2$ independent experiments ($n = 4$–6 mice/group in each experiment). Dashed lines indicate the limit of detection of each plaque assay. Statistical significance was determined by Student's t-test; ns not significant.

respectively. A common feature of each approach was the use of mouse cells, ensuring species compatibility with any additional intracellular proteins that might be required for mGBPchr3-mediated antiviral activity. Given the strong induction of multiple mGBPchr3 in ATII and AM following IAV infection, we were surprised that we did not observe any impact of mGBPchr3 on virus growth in any of our in vitro studies. While overexpression of a single mGBP may not be appropriate for optimal antiviral activity (e.g. if formation of mGBP heterodimers and/or complexing with other cellular proteins is required), we reasoned that subsequent studies using primary cells from WT or mGBPchr3 KO mice, including following pre-treatment with type I IFN to promote induction of mGBPs and other ISG proteins, should have provided favourable conditions to observe any antiviral effects mediated collectively by endogenous mGBPchr3 proteins. Indeed, we confirmed IFN-induced upregulation of individual mGBPchr3 in LA-4 cells (Fig. 1c), MLF (Fig. 4b) and BMDM (Fig. 5b) used in our studies. Given that we did not obtain evidence for mGBPchr3 inhibiting growth of any virus tested, we confirmed that DOX-inducible overexpression of either mGBP2 or mGBP5 in LA-4 cells inhibited growth of intracellular *E. coli* and that compared to BMDM from WT mice, growth of *E. coli* was significantly enhanced in mGBPchr3 KO BMDMs (Fig. 4). These findings confirmed the functionality of mGBPchr3 in the in vitro systems used in our studies. Recent studies from our group also confirmed that

mGBPchr3 KO MLFs or BMDMs infected with *M. catarrhalis* harboured increased numbers of intracellular bacteria compared to their WT counterparts[29].

Parenchymal cells represent primary targets for productive virus infection and amplification. Compared to ATII cells (RNA-seq, IAV-infected mice), distinct parenchymal cell types were used for in vitro infection and growth studies (mouse LA-4 cell line and WT and mGBPchr3 KO MLF) and both supported growth of each of the five viruses tested. Our original aim was to assess virus growth as a readout to identify mGBPchr3 KO with antiviral activity, such that subsequent studies could focus on examining the impact of one or more mGBPs on preceding steps in the virus replication cycle (e.g. virus entry, genomic replication, viral protein production). Given that each virus grew to similar titres in WT versus mGBPchr3 MLF, even in MLF pre-treated with type I IFN prior to infection (two different MOI per virus), we did not perform additional experiments to examine earlier steps in the replication cycle of each virus. Moreover, while different viruses elicited a distinct spectrum of inflammatory mediators from MLF, no major differences were noted following infection of WT versus mGBPchr3 KO cells, even when cells were pre-treated with type I IFN prior to infection. Further refinement of in vitro studies could be performed to assess viral replication over time following low MOI infection (i.e. as the virus spread through cell monolayers) and/or by determing if IFN-γ priming of LA-4 cells with DOX-inducible expression of individual mGBPchr3 might enhance antiviral activity, as was observed for antibacterial activity in our studies (Fig. 3). Collectively, the results presented indicate that either individually (overexpression) or collectively (endogenous), mGBPchr3 do not mediate potent antiviral activity against IAV, HSV-1, LCMV, EMCV or SeV in the mouse parenchymal cells tested.

In addition to studies in MLFs, we also addressed the impact of mGBPchr3 during virus infection of BMDMs. This is of importance, given that macrophages and epithelial cells express different constitutive levels of mGBPchr3, as well as different induction patterns following IAV infection (Fig. 1). Moreover, most studies defining the inhibitory properties of mGBPs against intracellular bacteria and parasites have been performed using macrophages (reviewed in ref. 1). Consistent with previous reports[33,34], IAV and HSV-1 did not replicate productively in mouse BMDMs. Moreover, while LCMV, SeV and EMCV did grow in BMDM, no differences were noted between cells from WT or mGBPchr3 KO mice. Moreover, while one or more mGBPchr3 have been shown to promote inflammasome activation during bacterial infections[1,50–54], no differences in IAV-induced NLRP3 inflammasome activation were detected in BMDMs from mGBPchr3 KO mice compared to WT controls, noting that future studies could also assess inflammasome activation in response to other viruses, including HSV-1, LCMV, SeV and EMCV used in our studies. In these studies, we acknowledge that any effect mediated by specifically by mGBPchr3 in MLF or BMDM could be masked by the antiviral activities of other ISGs upregulated following IFN treatments. It is also possible that mGBPs expressed on chromosome 5 (*Gbp4*, *Gbp6*, *Gbp8*, *Gbp9*, *Gbp10*, *Gbp1)* could mediate antiviral activity in their own right and may even compensate for loss of mGBPchr3 in either cell type.

Mouse models are widely used to gain insights regarding pathogenesis and immunity to human IAV infections, including demonstrating the critical role of individual ISGs such as IFITM3[55], ISG15[56] and mMx1[57] in innate immunity to IAV. However, IAV infection of WT or mGBPchr3 KO mice resulted in similar titres of virus (in nose, lungs and BAL), as well as cellular inflammation in the BAL, at both early (3 dpi) and later (7 dpi) time points post-infection. Similarly, while we recently used the mouse zosteriform model to demonstrate the importance of mMx1 in limiting HSV-1 infection in vivo[26], no differences were noted in viral titres recovered from the skin or primary DRG of HSV-1-infected WT or mGBPchr3 KO mice, or in the spleen, lung and liver of LCMV-infected mice after intraperitoneal infection. Previous studies have used the same mGBPchr3 KO mice to demonstrate the importance of GBPchr3 against *Toxoplasma gondii*[32] and *Legionella pneumophila*[58] in vivo. Thus, while mGBPchr3 are upregulated in the lung following IAV infection, mGBPchr3 do not appear to play a major role in host defence against IAV infections nor do they mediate potent antiviral activity against the diverse viruses tested in our studies.

Reports describing the antiviral properties of individual mGBPchr3, or the collective effect of the mGBPchr3 cluster are scarce and, to our knowledge, antiviral activities are yet to be reported for mGBPchr5 proteins. To date, the most definitive evidence of mGBPchr3 mediating antiviral activity is in the context of IFN-γ-mediated inhibition of MNV. Positive-sense RNA viruses like MNV rearrange host endomembranes to form vacuole-like structures in the cytoplasm for their replication, termed the replication complex (RC)[59] and MNV replication is inhibited by IFN-γ at the stage of RC formation[60], compared to type I IFNs that primarily inhibit MNV protein translation[61]. A number of studies have demonstrated the importance of mGBPchr3 and, in particular, mGBP2 in targeting MNV RC to mediate IFN-γ-mediated control of MNV infection. Compared to WT BMDM, MNV replication was inhibited less efficiently by IFN-γ pre-treatment compared to mGBPchr3 KO BMDM and expression of mGBP2 in mGBPchr3 KO BMDM restored IFN-γ-mediated control of MNV replication[20]. Stable mGBP2 overexpression in RAW264.7 macrophages enhanced IFN-γ-mediated inhibition of MNV replication, as well as in HEK293T cells expressing MNV receptor CD3001f[19]. To study mGBPchr3 specifically in the context of IFN-γ-mediated control of MNV infection in vivo, mGBPchr3 KO animals crossed on to type I IFN receptor deficient mice (*Ifnar*$^{-/-}$) were shown to be more susceptible to MNV infection than *Ifnar*$^{-/-}$ x mGBPchr3 heterozygote animals[20]. Thus, similar to mGBP-mediated inhibition of intracellular bacteria and parasites, mGBPchr3 can contribute to IFN-γ-mediated immunity to a virus such as MNV that replicates in cytosolic vacuole-like structures. Herein, our studies focused on the antiviral activities of mGBPchr3 in the context of constitutive or IFNα-induced expression in vitro, and by comparing WT and mGBPchr3 KO mice on an immunocompetent C57BL/6 background. Future studies could determine the contribution of mGBPchr3 to IFN-γ-mediated immunity against different viruses noting, for example, that IFN-γ is reported to be a weak inhibitor of HSV-1 replication in vitro[62], and that IFN-γ-mediated immunity has little impact on IAV replication in mice[63] and, in some instances, might actually promote spread of IAV in mouse airways[64].

Overall, we conclude that mGBPchr3 are upregulated in airway macrophages and epithelial cells following IAV infection of mice, however they do not play a major role in restricting IAV replication in vitro or in vivo. Moreover, results clearly indicate that mGBPchr3 do not mediate potent antiviral activity against additional viruses such as HSV-1, LCMV, EMCV or SeV in mouse parenchymal cells or BMDM, nor do mGBPchr3 KO mice show increased susceptibility to HSV-1 or LCMV infections. Aside from MNV, it is interesting to note that other studies generally report only modest inhibition of virus growth by mGBPchr3. For example, Pan et al. reported significantly increased titres of DENV released 24 hpi from RAW264.7 macrophages following in vitro silencing of mGBP1[16], although actual virus titres reported were < 5 versus ~15 plaques in total, which is not indicative of a potent antiviral effect. Similarly, constitutive overexpression of mGBP2 in NIH 3T3 cells reduced titres of VSV and EMCV to ~48% and ~42%, respectively, compared to control cells (i.e. approximately 2-fold), noting that results were presented as 'percent of control' and actual virus titres were not shown[17]. Following on from our recent report that mGBP1 did not inhibit IAV infection in vitro or in a mouse model of infection[21], we now demonstrate that collectively, mGBPchr3 do not inhibit growth of IAV, HSV-1, LCMV, SeV or EMCV in vitro, nor do they inhibit IAV, HSV-1 or LCVM replication in vivo.

When considering dynamin-like GTPases, human and mouse Mx proteins are known to mediate potent antiviral activity, although there is little evidence that they inhibit intracellular bacteria or parasites. In contrast, the role of human and mouse GBPs in immunity to intracellular bacteria and parasites has been intensively studied (reviewed in ref. 1), although less is known regarding their role in antiviral immunity, particularly in vivo. However, a growing number of studies have reported the ability of particular hGBPs to inhibit different viruses in vitro, whereas few reports have

convincingly reported the ability of mGBPs to mediate potent antiviral activity in vitro or in vivo. For bacteria or parasites, hGBPs and mGBPs play major roles in inducing vacuolar rupture and bacteriolysis, thereby liberating bacterial antigens to activate the cytosolic inflammasome (reviewed in ref. 35). While certain hGBPs have been reported to inhibit virus infections, the mechanisms by which they exert antiviral activity appear to be quite different. For example, hGBP1 repressed genomic replication of VSV[65], disrupted actin filaments to inhibit nuclear delivery of KSHV[10] and targeted the viral capsid protein of hepatitis E virus to the lysosomal compartment resulting in virus inactivation[66]. In contrast, hGBP2 and hGBP5 have been reported to express broad antiviral activity, acting to inhibit furin-mediated maturation of diverse viral envelope glycoproteins[14,15]. Thus, the antimicrobial activities of GBPs against different intracellular bacteria and parasites share similar general features, but the antiviral activities appear to be quite diverse. Of note, none of the viruses utilized in our studies exhibit furin-dependent replication and it is possible that mGBPs might mediate antiviral activity against other viruses where furin-mediated processing is required to facilitate virion maturation. Moreover, given that some viruses have been reported to encode proteins which antagonize specific GBPs (e.g. the antiviral activity of human GBP1 was reported to be antagonized by the NS5A protein of CSFV[11] and the NS1 protein of IAV[13]) it is possible that the lack of antiviral activity observed in our studies might represent effective antagonism of one or more mGBPchr3 by certain viruses. In addition to their role in IFN-γ-mediated inhibition of MNV, it remains to be determined if specific viruses can be identified that are particularly sensitive to inhibition by one or more mGBPs in vitro and in vivo.

Methods

Cell lines and viruses

Mouse airway epithelial LA-4 cells (American Type Culture Collection (ATCC) CCL-196™) were maintained and passaged in Ham's F-12K (Kaighn's) medium (Gibco) containing 10% (v/v) foetal calf serum (FCS, Sigma-Aldrich, USA) and supplemented with 2 mM L-glutamine, 100 Units (U)/mL penicillin and 100 µg/mL of streptomycin (Gibco-BRL, NY) (F-12K$_{10}$). Madin-Darby Canine Kidney (MDCK) cells (ATCC CCL- 34) were maintained and passaged in RPMI 1640 medium containing 10% (v/v) FCS and supplemented as described above. 293 T cells (ATCC CRL-3216), Vero cells (CSL, Parkville, Australia) were maintained and passaged in Dulbecco's Modified Eagle Medium (DMEM) (Gibco) containing 10% (v/v) FCS and supplements (DMEM$_{10}$). Primary mouse lung fibroblasts (MLF) and bone marrow-derived macrophages (BMDM) were generated and cultured as described in ref. 21.

IAV (strain HKx31), a high-yielding reassortant of A/Aichi/2/1968 (H3N2) with PR8, and SeV (Cantell strain, from Dr Ashley Mansell, Hudson Institute of Molecular Research, Melbourne), were propagated in embryonated hen's eggs by standard procedures. Stocks of HSV-1 (KOS strain) and LCMV (Armstrong strain, from Prof. Scott Mueller, Department of Microbiology and Immunology, The University of Melbourne) and EMCV (from Prof. Paul Hertzog, Monash University, Australia), were all propagated in Vero cells. Titres of infectious virus were determined by standard plaque assay or Virsospot (VS) immunoassay (described below) and expressed as plaque-forming units (PFU)/mL or Virospot (VS)/mL, respectively.

LA-4 cell lines with doxycycline-inducible expression of intracellular proteins

Production of lentiviruses for the generation of LA-4 cell lines with doxycycline (DOX) inducible expression of mGBP1, 2, 3, 5 or 7 (Genebank accession numbers NM_010259.2, NM_010260.1, NM_001289492, NM_153564 and BK005760, respectively), each engineered to express an N-terminal FLAG-tag, or cytoplasmic hen egg ovalbumin lacking the sequence for cell surface trafficking as a control (CTRL), was performed as recently described for mGBP1[21]. After transduction, LA-4 cells were sorted based on mCherry positive cells using a FACSAria III instrument (BD Biosciences, New Jersey, USA). Cells cultured for 24 hr in the presence or absence of 1 µg/mL DOX were fixed, stained with fixable viability dye eFluor 780 (eBioscience) and then permeabilised and stained with APC-conjugated anti-FLAG mAb (clone L5, Biolegend), before analysis by flow cytometry.

Real-time qRT-PCR analysis

RNA was extracted from mouse cells using the RNeasy Mini Kit (Qiagen, Germany) according to the manufacturer's instructions. RNA purity and quantity were determined by nanodrop (Thermoscientific, USA). Total RNA was reverse transcribed into cDNA using SensiFAST cDNA Synthesis Kit (Bioline, United Kingdom). SensiFAST™ SYBR® Lo-ROX kit (Bioline) was used with primers for individual mGBPchr3 as described in ref. 29 and data were analyzed with a QuantStudio 7 Flex RT-PCR System (Applied Biosystems). Relative gene expression of mGBPchr3 was normalized to mouse GAPDH, then expressed as a fold change from mock/untreated using the $2^{-\Delta\Delta CT}$ method.

In vitro infections for virus infectivity titrations and analysis of soluble inflammatory mediators

Cells seeded into 12-well tissue culture plates (Corning, NY) were cultured overnight at 37 °C, 5% (v/v) CO_2 in a humidified incubator prior to experiments. The next day, viable cell counts performed to calculate the multiplicity of infection (MOI) of each virus. For viral infection, cell monolayers were washed once with serum-free media and incubated with 1 mL per well of virus diluted in serum-free media. After 60 min at 37 °C, cells were washed three times and cultured at 37 °C for 2–48 hpi. For virus growth experiments, supernatants were clarified by centrifugation (2000 × g for 5 min) and stored at −80 °C prior to titration by plaque assay or VS assay (see below). To assess levels of inflammatory mediators, a BD™ cytometric bead array (CBA) mouse anti-virus response panel kit (CBA; BD Biosciences, San Diego, CA) was used to determine levels of IFN-γ, CXCL1, TNF-α, CCL2, IL-12, CCL2, IL-1β, CXCL10, GM-CSF, IL-10, IFN-β, IFN-α and IL-6 in clarified supernatants, as per the manufacturer's instructions. Analyte concentration was expressed as pg/mL ± standard deviation (SD).

Plaque assays and Virospot assays to determine titres of infectious virus

Titres of infectious IAV were determined by standard plaque assay or by Virospot (VS) immunostain assay on MDCK cells as described[21]. Titres of infectious HSV-1, EMCV and LCMV were determined by standard plaque assay on Vero cells[67]. HEp-2 cells (obtained from the ATCC (CCL-23) and confirmed negative for mycoplasma) are widely used to determine infectivity titres of SeV and LCMV and were used in VS assays in our studies. Briefly, cells (4×10^4 cells/well in 100 µL) seeded into a flat-bottomed 96-well tissue culture plates (Corning, NY) were incubated overnight, washed in serum-free media and then incubated with 10-fold dilutions of cell-free virus samples (100 µL) prepared in serum-free media. After 1 hr at 37 °C, 100 µL of overlay media (equal volumes of 6.4% (w/v) carboxymethylcellulose sodium salt (CMC) (Sigma-Aldrich) and 2x MEM media (Sigma-Aldrich)) was added, noting that for SeV titration the overlay also contained with 2 µg/mL TPCK-treated trypsin. After 48 h, overlay was removed and monolayers were fixed with cold 80% (v/v) acetone for 10 min on ice. For staining, wells were incubated with 200 µL blocking solution (5% (w/v) skim milk in PBS containing 0.05% (v/v) Tween 20 (Sigma-Aldrich)) for 30 min, then incubated with chicken anti-SeV polyclonal antibody (Abcam) or rat anti-LCMV nucleoprotein mAb (clone VL-4, Biocell) for SeV or LCMV, respectively, for 30 min at 37 °C. Plates were then washed three times with PBS containing 0.05% (v/v) Tween 20, then incubated with horseradish peroxidase (HRP)–conjugated rabbit anti-mouse (Dako) or goat anti-rat (Thermo Fisher Scientific) antibodies. After washing, plates were air-dried and incubated with KPL TrueBlue™ Peroxidase Substrate (Life sciences Inc., Milford, MA, USA) at RT in the dark, washed in water then air-dried and scanned using a CTL ImmunoSpot analyser (CTL, OH, USA) with CTL Switchboard 2.6.0 (x86). Spots (10-200/well) were counted manually using ImageJ Cell Counter software and 10 spots/well in the neat sample was set as the lower limit of detection (LLOD). Samples below this

LLOD were assigned an arbitrary value of 9 for calculations and for statistical analyses. Negative (media alone) and positive (virus stock) controls were included in all VS assays, and titres of infectious virus were expressed as VS/mL of original sample.

Assessing IAV-induced inflammasome activation in murine bone-marrow derived macrophages (BMDMs)

BMDMs were seeded in antibiotic-free media in 12-well plates. To activate the inflammasome, BMDMs were infected with IAV (HKx31; MOI 25) in serum-free media and supplemented with 10% vol/vol FCS 2 hpi. To activate the canonical NLRP3 inflammasome as a control, BMDMs were primed with 500 ng/mL ultrapure LPS from *E. coli* (Enzo Life Sciences) for 3 h and stimulated with 5 mM ATP (Roche) for 45 min. Cell culture supernatants and cell lysates were collected for lactate dehydrogenase (LDH), cytokine and immunoblotting analyses at 16 hpi. Levels of LDH released by cells were determined using a CytoTox 96 Non-Radioactive Cytotoxicity Assay according to the manufacturer's instructions (Promega). Cytokine levels were determined using a multiplex ELISA kit (Millipore) and an IL-18 ELISA kit (ThermoFisher) according to the manufacturer's instructions. Caspase-1 and gasdermin D protein were detected in BMDM lysates by western blotting using the primary antibodies AG-20B-0042, Adipogen and ab209845, Abcam, respectively, in conjunction with HRP-conjugated secondary antibody and Clarity Western ECL substrate (BioRad) and the ChemiDoc Touch Imaging System (BioRad).

Quantification of viable intracellular E. coli

E coli (1175, ATTC) and GFP-*E. coli* (25922, ATTC) were grown as described previously[31]. LA-4 cells were cultured overnight in media with 1 μg/mL DOX. LA-4 cells were further left untreated or treated with 100 U/mL of mouse IFN-g for another 24 h. Media were then removed and replenished with F-12K media supplemented with 10% FBS without antibiotics. LA-4 cells were then infected with GFP-*E. coli* (MOI 20) for 1 h followed by incubation with gentamicin (50 μg/mL) for 1 h to kill extracellular bacteria. After washing, LA-4 cells were monitored using the IncuCyte Zoom imaging system (Essen Biosciences) to track the number of intracellular GFP-*E. coli* for 2 h, 4 h, 8 h and 12 h post infection. Data from 4 h, 8 h and 12 h were normalized to the 2 h timepoint set at 100%. To determine the sensitivity of *E. coli* to DOX treatment, LA-4 cells were cultured overnight in media with or without 1 μg/mL DOX. LA-4 cells were further left untreated or treated with 100 U/mL of mouse IFN-g for another 24 h. Media were then removed and replenished with F-12K media supplemented with 10% FBS without antibiotics. LA-4 cells were infected with GFP-*E. coli* (MOI 20) for 7 h followed by incubation with gentamicin (50 μg/mL) for 1 h to kill extracellular bacteria (total 8 h). After washing, LA-4 cells were monitored immediately using the IncuCyte Zoom imaging system (Essen Biosciences) to track the number of intracellular GFP-*E. coli*. Data from LA-4 cells expressing mGBP2 or mGBP5 were normalized to LA-4 cells expressing OVA set at 100%.

Infection of mice with IAV, HSV-1 or LCMV

Heterozygote mGBPchr3 KO mice obtained from Osaka University[32] were bred to generate homozygous WT and GBPchr3 KO mice to ensure consistent genetic background. Mice were bred and housed in specific pathogen-free conditions in the Bioresources Facility of the Peter Doherty Institute for Infection and Immunity, Melbourne, Australia. All research complied with the University of Melbourne's Animal Experimentation Ethics guidelines and policies, and all experimental protocols were approved by the University of Melbourne Animal Ethics Committee (Approval numbers 1814689 & 23262).

For IAV infection, mice (6-10 weeks) were anaesthetized and infected with 10^4 PFU of IAV (HKx31) in 50 μL of PBS via the intranasal route. At 3 or 7 days post infection (dpi), bronchoalveolar lavage (BAL), lung and nasal tissue samples were collected as described in ref. 68. Plaque assay was used to determine titres of infectious virus in clarified homogenates prepared from the lungs and nasal tissues of IAV-infected mice and BD™ CBA mouse anti-virus response panel kit was used to determine levels of inflammatory mediators in cell-free BAL by flow cytometry. Phenotyping of single cell suspensions prepared from the BAL of IAV-infected mice was used to enumerate neutrophils (Ly6G$^+$, CD11b$^+$), eosinophils (Siglec-F$^+$, CD11b$^+$, CD64$^-$), NK cells (NK1.1$^+$, CD3$^-$), alveolar macrophages (CD64$^+$, Siglec-F$^+$, CD11c$^+$), pan-macrophages (CD64$^+$, Siglec-F$^-$, CD11b$^+$), pan-dendritic cells (pan-DC, CD64$^-$, CD11c$^+$, MHC II$^+$, CD24$^+$), CD4$^+$ T cells (CD3$^+$, CD4$^+$) and CD8$^+$ T cells (CD3$^+$, CD8$^+$) by flow cytometry, as described in ref. 21. In some experiments, cells were stained with PE- or APC-labelled DbPA224 (acid polymerase; SSLENFRAYV) or DbNP366 (nucleoprotein; ASNENMETM)-specific MHC-I tetramers before staining with anti-CD8 mAb[21].

HSV-1 flank infection of mice was performed using a flank scarification method described previously[26]. Briefly, mice (6–10 weeks) were anaesthetized, the left flank was shaved and depilated and a small area of skin (2–4 mm^2) situated above the dorsal tip of the spleen was scarified using a MultiPro Dremel drill (Dremel, Racine, USA) with a grindstone tip attachment (3.2 mm), held on the skin for 20 s(s). A 10 μL drop containing 10^6 PFU of HSV-1 (KOS) in PBS was applied to the abraded inoculation site, rubbed in and mice were bandaged for 48 h after virus application. At 3 or 5 dpi, mice were euthanised and skin and dorsal root ganglia (DRG) removed as described in ref. 26. A 1 × 1 cm piece of skin was removed from the primary site of inoculation into 1 mL serum-free media and a 1 × 2 cm piece of skin was taken from the secondary site (lower flank between the excised primary site and the anterior midline) into 1 ml serum free media, with a 0.5 cm section of skin left intact between the two excised sites. Mice were then perfused with PBS through the left ventricle and DRGs innervating the infected dermatome (Thoracic (T) 8–12) were removed with the aid of a dissecting microscope. All DRGs from one mouse were pooled into 1 mL of serum-free media. Skin and DRG samples were then homogenized and titres of infectious virus in clarified tissue samples was determined using standard plaque assays on Vero cells.

Mice received a single intraperitoneal (i.p.) injection with 10^6 PFU of LCMV Armstrong in 200 μL and at 3 dpi, mice were euthanised for collection of spleen and kidney. Clarified tissue homogenates were prepared for all organs, and titres of infectious virus determined by plaque assay on Vero cells as described above.

Data analysis, statistics and reproducibility

Flow cytometry data was analysed using FlowJo software, version 10.7.1 (Becton, Dickinson and Company, NJ, USA). Western blot images were analysed using ImageJ software, version 2.1.0/1.53c. Graphs and statistical analysis were performed using GraphPad Prism Version 9.2.0 (GraphPad software, CA, USA) and statistical significance was determined by Student's t-test or one-way ANOVA as indicated. Information regarding technical replicates and reproducibility (i.e. the number of independent experiments performed) are shown in each figure legend. Data are shown as means ± standard deviation (SD).

Reporting summary

Further information on research design is available in the Nature Portfolio Reporting Summary linked to this article.

Data availability

RNA-seq data (Supplementary Fig. 1) available via NCBI GEO database: accession number GSE115904. Source data for all figures is available in Supplementary Data 1. All other data are available from the corresponding author (or other sources, as applicable) on reasonable request.

Received: 9 November 2023; Accepted: 16 August 2024;
Published online: 25 August 2024

References

1. Man, S. M., Place, D. E., Kuriakose, T. & Kanneganti, T. D. Interferon-inducible guanylate-binding proteins at the interface of cell-

autonomous immunity and inflammasome activation. *J. Leukoc. Biol.* **101**, 143–150 (2017).
2. Vestal, D. J. & Jeyaratnam, J. A. The guanylate-binding proteins: emerging insights into the biochemical properties and functions of this family of large interferon-induced guanosine triphosphatase. *J. Interferon Cytokine Res.* **31**, 89–97 (2011).
3. Ghosh, A., Praefcke, G. J., Renault, L., Wittinghofer, A. & Herrmann, C. How guanylate-binding proteins achieve assembly-stimulated processive cleavage of GTP to GMP. *Nature* **440**, 101–104 (2006).
4. Praefcke, G. J. et al. Identification of residues in the human guanylate-binding protein 1 critical for nucleotide binding and cooperative GTP hydrolysis. *J. Mol. Biol.* **344**, 257–269 (2004).
5. Wehner, M., Kunzelmann, S. & Herrmann, C. The guanine cap of human guanylate-binding protein 1 is responsible for dimerization and self-activation of GTP hydrolysis. *Febs J.* **279**, 203–210 (2012).
6. Britzen-Laurent, N. et al. Intracellular trafficking of guanylate-binding proteins is regulated by heterodimerization in a hierarchical manner. *PLoS One* **5**, e14246 (2010).
7. Praefcke, G. J. K. Regulation of innate immune functions by guanylate-binding proteins. *Int. J. Med. Microbiol.* **308**, 237–245 (2017).
8. Anderson, S. L., Carton, J. M., Lou, J., Xing, L. & Rubin, B. Y. Interferon-induced guanylate binding protein-1 (GBP-1) mediates an antiviral effect against vesicular stomatitis virus and encephalomyocarditis virus. *Virology* **256**, 8–14 (1999).
9. Zhang, R., Li, Z., Tang, Y.-D., Su, C. & Zheng, C. When human guanylate-binding proteins meet viral infections. *J. Biomed. Sci.* **28**, 17 (2021).
10. Zou, Z. et al. Guanylate-Binding Protein 1 Inhibits Nuclear Delivery of Kaposi's Sarcoma-Associated Herpesvirus Virions by Disrupting Formation of Actin Filament. *J. Virol.* **91**, e00632–00617 (2017).
11. Li, L. F. et al. Guanylate-Binding Protein 1, an Interferon-Induced GTPase, Exerts an Antiviral Activity against Classical Swine Fever Virus Depending on Its GTPase Activity. *J. Virol.* **90**, 4412–4426 (2016).
12. Nordmann, A., Wixler, L., Boergeling, Y., Wixler, V. & Ludwig, S. A new splice variant of the human guanylate-binding protein 3 mediates anti-influenza activity through inhibition of viral transcription and replication. *Faseb J.* **26**, 1290–1300 (2012).
13. Zhu, Z. et al. Nonstructural protein 1 of influenza A virus interacts with human guanylate-binding protein 1 to antagonize antiviral activity. *PLoS One* **8**, e55920 (2013).
14. Braun, E. et al. Guanylate-Binding Proteins 2 and 5 Exert Broad Antiviral Activity by Inhibiting Furin-Mediated Processing of Viral Envelope Proteins. *Cell Rep.* **27**, 2092–2104.e2010 (2019).
15. Mesner, D. et al. SARS-CoV-2 evolution influences GBP and IFITM sensitivity. *Proc. Natl Acad. Sci. USA* **120**, e2212577120 (2023).
16. Pan, W., Zuo, X., Feng, T., Shi, X. & Dai, J. Guanylate-binding protein 1 participates in cellular antiviral response to dengue virus. *Virol. J.* **9**, 292–298 (2012).
17. Carter, C. C., Gorbacheva, V. Y. & Vestal, D. J. Inhibition of VSV and EMCV replication by the interferon-induced GTPase, mGBP-2: differential requirement for wild-type GTP binding domain. *Arch. Virol.* **150**, 1213–1220 (2005).
18. Janzen, C., Kochs, G. & Haller, O. A monomeric GTPase-negative MxA mutant with antiviral activity. *J. Virol.* **74**, 8202–8206 (2000).
19. Yu, P. et al. Guanylate-binding protein 2 orchestrates innate immune responses against murine norovirus and is antagonized by the viral protein NS7. *J. Biol. Chem.* **295**, 8036–8047 (2020).
20. Biering, S. B. et al. Viral Replication Complexes Are Targeted by LC3-Guided Interferon-Inducible GTPases. *Cell Host Microbe* **22**, 74–85.e77 (2017).
21. Tessema, M. B. et al. Mouse guanylate-binding protein 1 does not mediate antiviral activity against influenza virus in vitro or in vivo. *Immunol. Cell Biol.* **n/a 101** 383–396 (2023).
22. Ma, J. Z. et al. Unique transcriptional architecture in airway epithelial cells and macrophages shapes distinct responses following influenza virus infection ex vivo. *J. Virol.* **93**, e01986–18 (2019).
23. Villalon-Letelier, F., Farrukee, R., Londrigan, S. L., Brooks, A. G. & Reading, P. C. Isoforms of Human MARCH1 Differ in Ability to Restrict Influenza A Viruses Due to Differences in Their N Terminal Cytoplasmic Domain. *Viruses* **14**, 2549 (2022).
24. Villalon-Letelier, F., Brooks, A. G., Londrigan, S. L. & Reading, P. C. MARCH8 Restricts Influenza A Virus Infectivity but Does Not Downregulate Viral Glycoprotein Expression at the Surface of Infected Cells. *mBio* **12**, e0148421 (2021).
25. Meischel, T. et al. IFITM proteins that restrict the early stages of respiratory virus infection do not influence late-stage replication. *J. Virol.* **95**, Jvi0083721 (2021).
26. Tessema, M. B. et al. Mouse Mx1 Inhibits Herpes Simplex Virus Type 1 Genomic Replication and Late Gene Expression In Vitro and Prevents Lesion Formation in the Mouse Zosteriform Model. *J. Virol.* **96**, e0041922 (2022).
27. Livak, K. J. & Schmittgen, T. D. Analysis of relative gene expression data using real-time quantitative PCR and the 2(-Delta Delta C(T)) Method. *Methods* **25**, 402–408 (2001).
28. Haldar, A. K. et al. Guanylate Binding Proteins Restrict Leishmania donovani Growth in Nonphagocytic Cells Independent of Parasitophorous Vacuolar Targeting. *mBio* **11**, e01464–01420 (2020).
29. Enosi Tuipulotu, D. et al. Immunity against Moraxella catarrhalis requires guanylate-binding proteins and caspase-11-NLRP3 inflammasomes. *EMBO J.* **42**, e112558 (2023).
30. Man, S. M. et al. The transcription factor IRF1 and guanylate-binding proteins target activation of the AIM2 inflammasome by Francisella infection. *Nat. Immunol.* **16**, 467–475 (2015).
31. Feng, S. et al. Pathogen-selective killing by guanylate-binding proteins as a molecular mechanism leading to inflammasome signaling. *Nat. Commun.* **13**, 4395 (2022).
32. Yamamoto, M. et al. A cluster of interferon-gamma-inducible p65 GTPases plays a critical role in host defense against Toxoplasma gondii. *Immunity* **37**, 302–313 (2012).
33. Londrigan, S. L. et al. Infection of Mouse Macrophages by Seasonal Influenza Viruses Can Be Restricted at the Level of Virus Entry and at a Late Stage in the Virus Life Cycle. *J. Virol.* **89**, 12319–12329 (2015).
34. Mott, K. R., UnderHill, D., Wechsler, S. L., Town, T. & Ghiasi, H. A role for the JAK-STAT1 pathway in blocking replication of HSV-1 in dendritic cells and macrophages. *Virol. J.* **6**, 56 (2009).
35. Ngo, C. C. & Man, S. M. Mechanisms and functions of guanylate-binding proteins and related interferon-inducible GTPases: Roles in intracellular lysis of pathogens. *Cell Microbiol.* **19**, e12791 (2017).
36. Kovarova, M. et al. NLRP1-dependent pyroptosis leads to acute lung injury and morbidity in mice. *J. Immunol.* **189**, 2006–2016 (2012).
37. Wojtasiak, M. et al. Gr-1+ cells, but not neutrophils, limit virus replication and lesion development following flank infection of mice with herpes simplex virus type-1. *Virology* **407**, 143–151 (2010).
38. Olson, M. R., McDermott, D. S. & Varga, S. M. The initial draining lymph node primes the bulk of the CD8 T cell response and influences memory T cell trafficking after a systemic viral infection. *PLoS Pathog.* **8**, e1003054 (2012).
39. Degrandi, D. et al. Murine guanylate binding protein 2 (mGBP2) controls Toxoplasma gondii replication. *Proc. Natl Acad. Sci. USA* **110**, 294–299 (2013).
40. Melzer, T., Duffy, A., Weiss, L. M. & Halonen, S. K. The gamma interferon (IFN-gamma)-inducible GTP-binding protein IGTP is necessary for toxoplasma vacuolar disruption and induces parasite egression in IFN-gamma-stimulated astrocytes. *Infect. Immun.* **76**, 4883–4894 (2008).
41. Cheng, Y. S., Colonno, R. J. & Yin, F. H. Interferon induction of fibroblast proteins with guanylate binding activity. *J. Biol. Chem.* **258**, 7746–7750 (1983).

42. Decker, T. et al. Interactions of alpha- and gamma-interferon in the transcriptional regulation of the gene encoding a guanylate-binding protein. *EMBO J.* **8**, 2009–2014 (1989).
43. Lew, D. J., Decker, T., Strehlow, I. & Darnell, J. E. Overlapping elements in the guanylate-binding protein gene promoter mediate transcriptional induction by alpha and gamma interferons. *Mol. Cell. Biol.* **11**, 182–191 (1991).
44. Degrandi, D. et al. Extensive characterization of IFN-induced GTPases mGBP1 to mGBP10 involved in host defense. *J. Immunol.* **179**, 7729–7740 (2007).
45. Boehm, U. et al. Two families of GTPases dominate the complex cellular response to IFN-gamma. *J. Immunol.* **161**, 6715–6723 (1998).
46. Corte-Real, J. V., Baldauf, H. M., Melo-Ferreira, J., Abrantes, J. & Esteves, P. J. Evolution of Guanylate Binding Protein (GBP) Genes in Muroid Rodents (Muridae and Cricetidae) Reveals an Outstanding Pattern of Gain and Loss. *Front Immunol.* **13**, 752186 (2022).
47. Olszewski, M. A., Gray, J. & Vestal, D. J. In silico genomic analysis of the human and murine guanylate-binding protein (GBP) gene clusters. *J. Interferon Cytokine Res* **26**, 328–352 (2006).
48. Kirkby, M., Enosi Tuipulotu, D., Feng, S., Lo Pilato, J. & Man, S. M. Guanylate-binding proteins: mechanisms of pattern recognition and antimicrobial functions. *Trends Biochem Sci.* **48**, 883–893 (2023).
49. Ngo, C. C. & Man, S. M. Mechanisms and functions of guanylate-binding proteins and related interferon-inducible GTPases: Roles in intracellular lysis of pathogens. *Cell Microbiol* **19**, https://doi.org/10.1111/cmi.12791 (2017).
50. Meunier, E. et al. Guanylate-binding proteins promote activation of the AIM2 inflammasome during infection with Francisella novicida. *Nat. Immunol.* **16**, 476–484 (2015).
51. Henry, T., Brotcke, A., Weiss, D. S., Thompson, L. J. & Monack, D. M. Type I interferon signaling is required for activation of the inflammasome during Francisella infection. *J. Exp. Med* **204**, 987–994 (2007).
52. Fernandes-Alnemri, T. et al. The AIM2 inflammasome is critical for innate immunity to Francisella tularensis. *Nat. Immunol.* **11**, 385–393 (2010).
53. Santos, J. C. et al. LPS targets host guanylate-binding proteins to the bacterial outer membrane for non-canonical inflammasome activation. *Embo j.* **37**, e98089 (2018).
54. Pilla, D. M. et al. Guanylate binding proteins promote caspase-11-dependent pyroptosis in response to cytoplasmic LPS. *Proc. Natl Acad. Sci. USA* **111**, 6046–6051 (2014).
55. Everitt, A. R. et al. IFITM3 restricts the morbidity and mortality associated with influenza. *Nature* **484**, 519–523 (2012).
56. Morales, D. J. et al. Novel mode of ISG15-mediated protection against influenza A virus and Sendai virus in mice. *J. Virol.* **89**, 337–349 (2015).
57. Shin, D. L., Hatesuer, B., Bergmann, S., Nedelko, T. & Schughart, K. Protection from Severe Influenza Virus Infections in Mice Carrying the Mx1 Influenza Virus Resistance Gene Strongly Depends on Genetic Background. *J. Virol.* **89**, 9998–10009 (2015).
58. Liu, B. C. et al. Constitutive Interferon Maintains GBP Expression Required for Release of Bacterial Components Upstream of Pyroptosis and Anti-DNA Responses. *Cell Rep.* **24**, 155–168.e155 (2018).
59. den Boon, J. A., Diaz, A. & Ahlquist, P. Cytoplasmic viral replication complexes. *Cell Host Microbe* **8**, 77–85 (2010).
60. Hwang, S. et al. Nondegradative role of Atg5-Atg12/ Atg16L1 autophagy protein complex in antiviral activity of interferon gamma. *Cell Host Microbe* **11**, 397–409 (2012).
61. Changotra, H. et al. Type I and Type II Interferons Inhibit the Translation of Murine Norovirus Proteins. *J. Virol.* **83**, 5683–5692 (2009).
62. Sainz, B. Jr. & Halford, W. P. Alpha/Beta interferon and gamma interferon synergize to inhibit the replication of herpes simplex virus type 1. *J. Virol.* **76**, 11541–11550 (2002).
63. Turner, S. J., Olivas, E., Gutierrez, A., Diaz, G. & Doherty, P. C. Disregulated influenza A virus-specific CD8+ T cell homeostasis in the absence of IFN-gamma signaling. *J. Immunol.* **178**, 7616–7622 (2007).
64. Nicol, M. Q. et al. Lack of IFNγ signaling attenuates spread of influenza A virus in vivo and leads to reduced pathogenesis. *Virology* **526**, 155–164 (2019).
65. Gu, T. et al. Tupaia guanylate-binding protein 1 interacts with vesicular stomatitis virus phosphoprotein and represses primary transcription of the viral genome. *Cytokine* **138**, 155388 (2021).
66. Glitscher, M. et al. Identification of the interferon-inducible GTPase GBP1 as major restriction factor for the Hepatitis E virus. *J. Virol.* **95**, e01564–20 (2021).
67. van Lint, A. et al. Herpes simplex virus-specific CD8+ T cells can clear established lytic infections from skin and nerves and can partially limit the early spread of virus after cutaneous inoculation. *J. Immunol.* **172**, 392–397 (2004).
68. Tate, M. D., Brooks, A. G. & Reading, P. C. The role of neutrophils in the upper and lower respiratory tract during influenza virus infection of mice. *Respir. Res* **9**, 57–69 (2008).

Acknowledgements

We acknowledge the Melbourne Cytometry Platform (Peter Doherty Institute node) for provision of flow cytometry services. We also thank Marco Herold at the Walter and Eliza Hall Institute for provision of the lentiviral constructs. This study was supported by Project Grant #APP1143154 from The National Health and Medical Research Council (NHMRC) of Australia. The Melbourne WHO Collaborating Centre for Reference and Research on Influenza is supported by the Australian Government Department of Health and Ageing.

Author contributions

Conceptualization, M.B.T., S.L.L, S.M.M., P.C.R.; methodology, M.B.T., D.E.T., S.F.; validation, M.B.T.; formal analysis, M.B.T., D.E.T., S.F., R.F., P.C.R.; investigation, F.V.L., S.F., D.E.T., C.G.G, P.C.R., C.N.; resources, A.G.B, S.L.L., Y.M., S.M.M., P.C.R.; data curation, M.B.T., S.F., D.E.T., P.C.R.; writing—original draft preparation, M.B.T., P.C.R; writing—review and editing, all authors; visualization, M.B.T., D.E.T.; supervision, A.G.B, S.L.L., D.T.U., P.C.R; project administration, A.G.B, S.L.L., P.C.R; funding acquisition, A.G.B, S.L.L., P.C.R. All authors have read and agreed to the published version of the manuscript.

Competing interests

Si Ming Man is an Editorial Board Member for *Communications Biology*, but was not involved in the editorial review of, nor the decision to publish this article. All other authors declare no competing interests.

Additional information

Supplementary information The online version contains supplementary material available at https://doi.org/10.1038/s42003-024-06748-8.

Correspondence and requests for materials should be addressed to Patrick C. Reading.

Peer review information *Communications Biology* thanks the anonymous reviewers for their contribution to the peer review of this work. Primary Handling Editors: Joao Valente.